

ENGINEERING OF BIOMATERIALS

INŻYNIERIA BIOMATERIAŁÓW

JOURNAL OF POLISH SOCIETY FOR BIOMATERIALS AND FACULTY OF MATERIALS SCIENCE AND CERAMICS AGH-UST

CZASOPISMO POLSKIEGO STOWARZYSZENIA BIOMATERIAŁÓW I WYDZIAŁU INŻYNIERII MATERIAŁOWEJ I CERAMIKI AGH

Number 162

Numer 162

Volume XXIV

Rok XXIV

OCTOBER 2021

PAŹDZIERNIK 2021

ISSN 1429-7248

PUBLISHER:

WYDAWCA:

**Polish Society
for Biomaterials
in Krakow**

Polskie
Stowarzyszenie
Biomateriałów
w Krakowie

**EDITORIAL
COMMITTEE:**

KOMITET

REDAKCYJNY:

Editor-in-Chief

Redaktor naczelny

Elżbieta Pamuła

Editor

Redaktor

Patrycja

Domalik-Pyzik

Secretary of editorial

Sekretarz redakcji

Design

Projekt

Katarzyna Trała

**ADDRESS OF
EDITORIAL OFFICE:**

ADRES REDAKCJI:

AGH-UST

30/A3, Mickiewicz Av.

30-059 Krakow, Poland

Akademia

Górnictwo-Hutnicza

al. Mickiewicza 30/A-3

30-059 Kraków

Issue: 250 copies

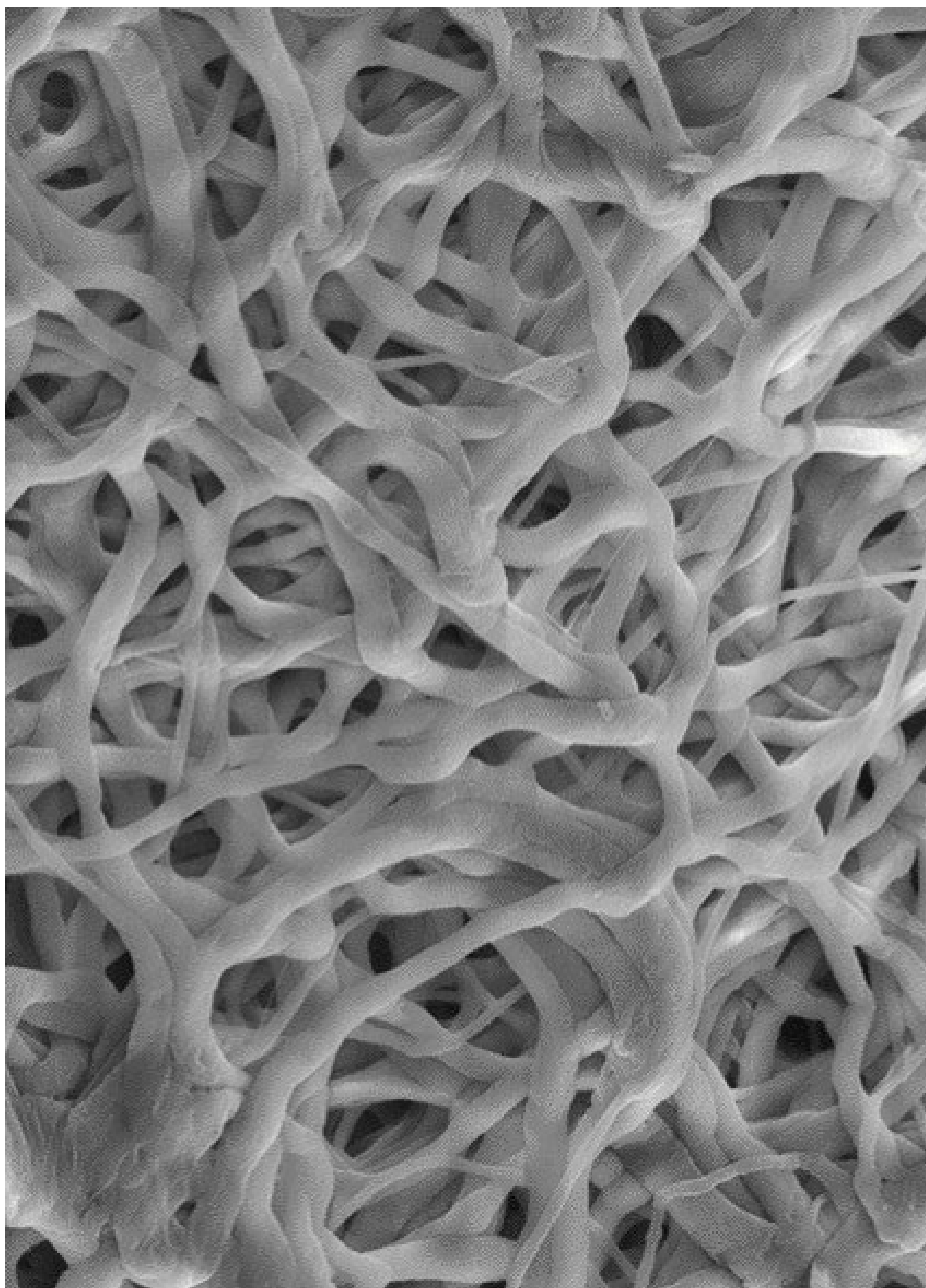
Nakład: 250 egz.

**Scientific Publishing
House AKAPIT**

Wydawnictwo Naukowe

AKAPIT

e-mail: wn@akapit.krakow.pl



EDITORIAL BOARD KOMITET REDAKCYJNY

EDITOR-IN-CHIEF

Elżbieta Pamuła - AGH UNIVERSITY OF SCIENCE AND TECHNOLOGY, KRAKOW, POLAND

EDITOR

Patrycja Domalik-Pyzik - AGH UNIVERSITY OF SCIENCE AND TECHNOLOGY, KRAKOW, POLAND

INTERNATIONAL EDITORIAL BOARD MIĘDZYNARODOWY KOMITET REDAKCYJNY

Iulian Antoniac - UNIVERSITY POLITEHNICA OF BUCHAREST, ROMANIA

Lucie Bacakova - ACADEMY OF SCIENCE OF THE CZECH REPUBLIC, PRAGUE, CZECH REPUBLIC

Romuald Będziński - UNIVERSITY OF ZIELONA GÓRA, POLAND

Marta Błażewicz - AGH UNIVERSITY OF SCIENCE AND TECHNOLOGY, KRAKOW, POLAND

Stanisław Błażewicz - AGH UNIVERSITY OF SCIENCE AND TECHNOLOGY, KRAKOW, POLAND

Wojciech Chrzanowski - UNIVERSITY OF SYDNEY, AUSTRALIA

Jan Ryszard Dąbrowski - BIAŁYSTOK TECHNICAL UNIVERSITY, POLAND

Timothy Douglas - LANCASTER UNIVERSITY, UNITED KINGDOM

Christine Dupont-Gillain - UNIVERSITÉ CATHOLIQUE DE LOUVAIN, BELGIUM

Matthias Eppele - UNIVERSITY OF DUISBURG-ESSEN, GERMANY

Robert Hurt - BROWN UNIVERSITY, PROVIDENCE, USA

James Kirkpatrick - JOHANNES GUTENBERG UNIVERSITY, MAINZ, GERMANY

Ireneusz Kotela - CENTRAL CLINICAL HOSPITAL OF THE MINISTRY OF THE INTERIOR AND ADMINSTR. IN WARSAW, POLAND

Małgorzata Lewandowska-Szumieł - MEDICAL UNIVERSITY OF WARSAW, POLAND

Jan Marciniak - SILESIA UNIVERSITY OF TECHNOLOGY, ZABRZE, POLAND

Ion N. Mihailescu - NATIONAL INSTITUTE FOR LASER, PLASMA AND RADIATION PHYSICS, BUCHAREST, ROMANIA

Sergey Mikhlovsky - UNIVERSITY OF BRIGHTON, UNITED KINGDOM

Stanisław Mitura - TECHNICAL UNIVERSITY OF LIBEREC, CZECH REPUBLIC

Piotr Niedzielski - TECHNICAL UNIVERSITY OF LODZ, POLAND

Abhay Pandit - NATIONAL UNIVERSITY OF IRELAND, GALWAY, IRELAND

Stanisław Pielka - WROCLAW MEDICAL UNIVERSITY, POLAND

Vehid Salih - UCL EASTMAN DENTAL INSTITUTE, LONDON, UNITED KINGDOM

Jacek Składzień - JAGIELLONIAN UNIVERSITY, COLLEGIUM MEDICUM, KRAKOW, POLAND

Andrei V. Stanishevsky - UNIVERSITY OF ALABAMA AT BIRMINGHAM, USA

Anna Ślósarczyk - AGH UNIVERSITY OF SCIENCE AND TECHNOLOGY, KRAKOW, POLAND

Tadeusz Trzaska - UNIVERSITY SCHOOL OF PHYSICAL EDUCATION, POZNAŃ, POLAND

Dimitris Tsipras - ARISTOTLE UNIVERSITY OF THESSALONIKI, GREECE

Wskazówki dla autorów

1. Prace do opublikowania w kwartalniku „Engineering of Biomaterials / Inżynieria Biomateriałów” przyjmowane będą wyłącznie w języku angielskim.
2. Wszystkie nadsyłane artykuły są recenzowane.
3. Materiały do druku prosimy przysyłać za pomocą systemu online (www.biomaterials.pl).
4. Struktura artykułu:
 - TYTUŁ • Autorzy i instytucje • Streszczenie (200-250 słów) • Słowa kluczowe (4-6) • Wprowadzenie • Materiały i metody • Wyniki i dyskusja • Wnioski • Podziękowania • Piśmiennictwo
5. Autorzy przesyłają pełną wersję artykułu, łącznie z ilustracjami, tabelami, podpisami i literaturą w jednym pliku. Artykuł w tej formie przesyłany jest do recenzentów. Dodatkowo autorzy proszeni są o przesłanie materiałów ilustracyjnych (rysunki, schematy, fotografie, wykresy) w oddzielnych plikach (format np. .jpg, .gif, .tiff, .bmp). Rozdzielczość rysunków min. 300 dpi. Wszystkie rysunki i wykresy powinny być czarno-białe lub w odcieniach szarości i ponumerowane cyframi arabskimi. W tekście należy umieścić odnośniki do rysunków i tabel.
6. Na końcu artykułu należy podać wykaz piśmiennictwa w kolejności cytowania w tekście i kolejno ponumerowany.
7. Redakcja zastrzega sobie prawo wprowadzenia do opracowań autorskich zmian terminologicznych, poprawek redakcyjnych, stylistycznych, w celu dostosowania artykułu do norm przyjętych w naszym czasopiśmie. Zmiany i uzupełnienia merytoryczne będą dokonywane w uzgodnieniu z autorem.
8. Opinia lub uwagi recenzentów będą przekazywane Autorowi do ustosunkowania się. Nie dostarczenie poprawionego artykułu w terminie oznacza rezygnację Autora z publikacji pracy w naszym czasopiśmie.
9. Za publikację artykułów redakcja nie płaci honorarium autorskiego.
10. Adres redakcji:
Czasopismo
„Engineering of Biomaterials / Inżynieria Biomateriałów”
Akademia Górniczo-Hutnicza im. St. Staszica
Wydział Inżynierii Materiałowej i Ceramiki
al. Mickiewicza 30/A-3, 30-059 Kraków
tel. (48) 12 617 44 48, 12 617 25 61
e-mail: epamula@agh.edu.pl, kabe@agh.edu.pl

Szczegółowe informacje dotyczące przygotowania manuskryptu oraz procedury recenzowania dostępne są na stronie internetowej czasopisma:

www.biomaterials.pl

Instructions for authors

1. Papers for publication in quarterly journal „Engineering of Biomaterials / Inżynieria Biomateriałów” should be written in English.
2. All articles are reviewed.
3. Manuscripts should be submitted to editorial office through online submission system (www.biomaterials.pl).
4. A manuscript should be organized in the following order:
 - TITLE • Authors and affiliations • Abstract (200-250 words) • Keywords (4-6) • Introduction • Materials and Methods • Results and Discussion • Conclusions • Acknowledgements • References
5. All illustrations, figures, tables, graphs etc. preferably in black and white or grey scale should be additionally sent as separate electronic files (format .jpg, .gif, .tiff, .bmp). High-resolution figures are required for publication, at least 300 dpi. All figures must be numbered in the order in which they appear in the paper and captioned below. They should be referenced in the text. The captions of all figures should be submitted on a separate sheet.
6. References should be listed at the end of the article. Number the references consecutively in the order in which they are first mentioned in the text.
7. The Editors reserve the right to improve manuscripts on grammar and style and to modify the manuscripts to fit in with the style of the journal. If extensive alterations are required, the manuscript will be returned to the authors for revision.
8. Opinion or notes of reviewers will be transferred to the author. If the corrected article will not be supplied on time, it means that the author has resigned from publication of work in our journal.
9. Editorial does not pay author honorarium for publication of article.
10. Address of editorial office:
Journal
„Engineering of Biomaterials / Inżynieria Biomateriałów”
AGH University of Science and Technology
Faculty of Materials Science and Ceramics
30/A-3, Mickiewicz Av., 30-059 Krakow, Poland
tel. (48) 12) 617 44 48, 12 617 25 61
e-mail: epamula@agh.edu.pl, kabe@agh.edu.pl

Detailed information concerning manuscript preparation and review process are available at the journal's website:

www.biomaterials.pl

STUDIA PODYPLOMOWE

Biomateriały – Materiały dla Medycyny

2021/2022

Organizator: Akademia Górniczo-Hutnicza im. Stanisława Staszica w Krakowie Wydział Inżynierii Materiałowej i Ceramiki Katedra Biomateriałów i Kompozytów	Adres: 30-059 Kraków, Al. Mickiewicza 30 Pawilon A3, p. 208, 210 tel. 12 617 44 48, 12 617 23 38, fax. 12 617 33 71 email: epamula@agh.edu.pl; krok@agh.edu.pl
Kierownik: prof. dr hab. inż. Elżbieta Pamuła Sekretarz: dr inż. Małgorzata Krok-Borkowicz	https://www.agh.edu.pl/ksztalcenie/oferta-ksztalcenia/studia-podyplomowe-kursy-dokształcające-i-szkolenia/biomateriały-materiały-dla-medycyny/
Charakterystyka: Tematyka prezentowana w trakcie zajęć obejmuje przegląd wszystkich grup materiałów dla zastosowań medycznych: metalicznych, ceramicznych, polimerowych, węglowych i kompozytowych. Słuchacze zapoznają się z metodami projektowania i wytwarzania biomateriałów a następnie możliwościami analizy ich właściwości mechanicznych, właściwości fizykochemicznych (laboratoria z metod badań: elektronowa mikroskopia skaningowa, mikroskopia sił atomowych, spektroskopia w podczerwieni, badania energii powierzchniowej i zwilżalności) i właściwości biologicznych (badania: <i>in vitro</i> i <i>in vivo</i>). Omawiane są regulacje prawne i aspekty etyczne związane z badaniami na zwierzętach i badaniami klinicznymi (norma EU ISO 10993). Słuchacze zapoznają się z najnowszymi osiągnięciami w zakresie nowoczesnych nośników leków, medycyny regeneracyjnej i inżynierii tkankowej.	
Sylwetka absolwenta: Studia adresowane są do absolwentów uczelni technicznych (inżynieria materiałowa, technologia chemiczna), przyrodniczych (chemia, biologia, biotechnologia) a także medycznych, stomatologicznych, farmaceutycznych i weterynaryjnych, pragnących zdobyć, poszerzyć i ugruntować wiedzę z zakresu inżynierii biomateriałów i nowoczesnych materiałów dla medycyny. Słuchacze zdobywają i/lub pogłębiają wiedzę z zakresu inżynierii biomateriałów. Po zakończeniu studiów wykazują się znajomością budowy, właściwości i sposobu otrzymywania materiałów przeznaczonych dla medycyny. Potrafią analizować wyniki badań i przekładać je na zachowanie się biomateriału w warunkach żywego organizmu. Ponadto słuchacze wprowadzani są w zagadnienia dotyczące wymagań normowych, etycznych i prawnych niezbędnych do wprowadzenia nowego materiału na rynek. Ukończenie studiów pozwala na nabycie umiejętności przygotowywania wniosków do Komisji Etycznych i doboru metod badawczych w zakresie analizy biogodności materiałów.	
Zasady naboru: Termin zgłoszeń: od 20.09.2021 do 20.10.2021 (liczba miejsc ograniczona - decyduje kolejność zgłoszeń) Wymagane dokumenty: dyplom ukończenia szkoły wyższej Osoby przyjmujące zgłoszenia: prof. dr hab. inż. Elżbieta Pamuła (pawilon A3, p. 208, tel. 12 617 44 48, e-mail: epamula@agh.edu.pl) dr inż. Małgorzata Krok-Borkowicz (pawilon A3, p. 210, tel. 12 617 23 38, e-mail: krok@agh.edu.pl)	
Czas trwania: 2 semestry (od XI 2021 r. do VI 2022 r.) 8 zjazdów (soboty-niedziele) raz w miesiącu przewidywana liczba godzin: 160	Opłaty: 3 000 zł (za dwa semestry)



31st Biomaterials in Medicine and Veterinary Medicine

Annual Conference

13 – 16 October 2022 Rytro, Poland

SAVE THE DATE

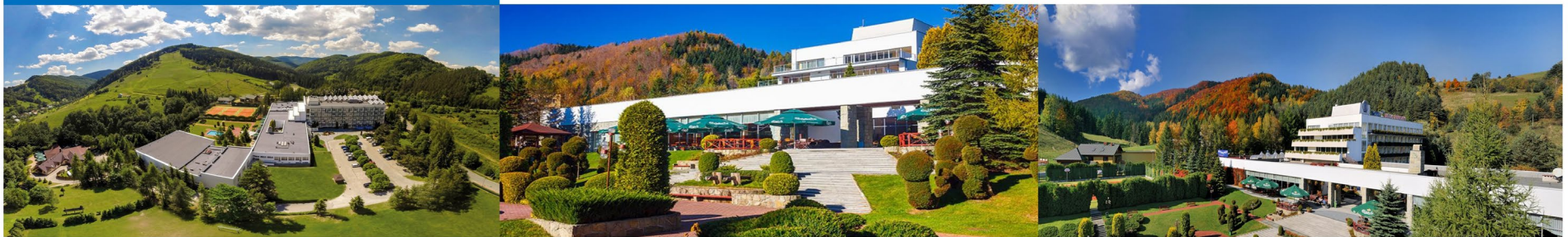
13-16

OCTOBER
2022

www.biomat.agh.edu.pl



REGISTER
AND
SUBMIT
AN ABSTRACT



SPIS TREŚCI CONTENTS

STRESS RELAXATION PHENOMENA IN POLYMERIC ORTHODONTIC LIGATURES GRZEGORZ MILEWSKI	2
POLY(SEBACIC ANHYDRIDE) MICROPARTICLES LOADED WITH CURCUMIN FOR PULMONARY PURPOSES KONRAD KWIECIEŃ, KATARZYNA RECZYŃSKA- KOLMAN, DARIA NIEWOLIK, KATARZYNA JASZCZ, ELŻBIETA PAMUŁA	7
PREPARATION AND PRELIMINARY <i>IN VIVO</i> STUDIES OF RESORBABLE POLYMER MODIFIED WITH ALLOGENIC BONE CHIPS FOR GUIDED BONE REGENERATION AND ORTHOPEDIC IMPLANTS BARBARA SZARANIEC, TOMASZ SZPONDER, KAROL GRYŃ, MACIEJ AMBROZIAK, GRZEGORZ GUT, ŁUKASZ KOPERSKI, JAN CHŁOPEK	13
EMULSION ELECTROSPINNING – METHOD TO INTRODUCE PROTEINS FOR BIOMEDICAL APPLICATIONS ROKSANA KURPANIK, ALICJA RAPACZ-KMITA, ANNA ŚCISŁOWSKA-CZARNECKA, EWA STODOLAK-ZYCH	20
ERRATUM	26

STRESS RELAXATION PHENOMENA IN POLYMERIC ORTHODONTIC LIGATURES

GRZEGORZ MILEWSKI* 

CRACOW UNIVERSITY OF TECHNOLOGY,
DEPARTMENT OF APPLIED MECHANICS AND BIOMECHANICS,
WARSZAWSKA 24, 31-155 KRAKOW, POLAND

*E-MAIL: GRZEGORZ.MILEWSKI@PK.EDU.PL

Abstract

Elastomeric products are applied in orthodontics mainly as elastic ligatures or chains and have become an alternative to wire ligation made of titanium alloy or stainless steel. Despite their popularity among the dentists and undoubtful advantages, some essential warnings are being raised regarding the degree of load loss. This relaxation phenomenon seems to be a dominant feature in the time-dependent behaviour of those elements in orthodontic procedures, such as dentition corrections or teeth extrusions. The aim of the paper was to examine and analyse the rheological properties of biocompatible orthodontic elastomeric ligatures. Five different polymeric orthodontic ligatures were examined in the following experiments: a simple relaxation test, relaxation simulating orthodontic extrusion and the two-steps relaxation process, which stands for so-called 'secondary tightening', resulting in the increase of the orthodontic force. The results of the relaxation experiments proved that among various descriptions of that phenomenon, the power-law descriptions fit the best time-dependent behaviour during orthodontic procedures. Power-law models give the most intensive initial relaxation, which is characteristic for elastomeric ligatures. The obtained results and analyses allow precise control of the treatment progress in the orthodontic extrusion procedure.

Keywords: orthodontic extrusion, polyurethane ligatures, stress relaxation, rheological models

[Engineering of Biomaterials 162 (2021) 2-6]

doi:10.34821/eng.biomat.162.2021.2-6



Copyright © 2021 by the authors. Some rights reserved.
Except otherwise noted, this work is licensed under
<https://creativecommons.org/licenses/by/4.0>

Introduction

Orthodontics is a part of dentistry which deals with the layout, arrangement, shape, and appearance of teeth in the oral cavity. Orthodontic treatment improves both the aesthetic image and the quality of dentition functioning. The controlled orthodontic extrusion induces the natural eruptive movement of the tooth towards the occlusal plane. This is achieved through the additional forces caused by polymeric flexible links as well as by fixed or movable metallic braces. Through the tooth, these forces affect both the periodontium and the alveolar bone, stimulating them to change and remodel [1-3]. Extrusion is also used as an auxiliary method preparing the teeth for endodontic treatment and further prosthetic procedures [4]. In the case of subgingival hard tissue cavities, it is an alternative to the tooth extraction.

This method allows to keep the patient's own root and associated periodontal ligaments.

Elastomeric products, mainly elastic ligatures and chains, are applied in orthodontic treatments in order to improve the aesthetic image and the quality of dentition functioning. For the first time, they were used in orthodontics several years ago as an alternative for a wire ligation made of stainless steel. They also replaced flexible teeth retraction appliances which were made of latex rubber and required daily replacement by the patient [5]. Despite their popularity among dentists and the undoubtful advantages, some essential warnings are being raised mainly concerning the degree of load loss due to the relaxation features in polymeric ligatures [6,7].

The aim of the paper was to examine and analyse the strength and rheological properties of biocompatible orthodontic elastomeric ligatures. Proper assessment of their rheological properties will enable dentists to predict the degree of load/stress loss due to the relaxation phenomenon in elastomeric ligatures. Finally, it will allow for precise control of the treatment progress in various orthodontic procedures.

Materials and Methods

Ligatures and chains are made of polyurethanes, which are elastomers able to bind under the influence of temperature, having - (NH) - (C = O) - O - as a structural unit and undergoing a sequential condensation polymerization reaction. Ligatures of the 0.2-0.36 mm diameter range are commonly used in dentistry [3]. Polymers characterized with rubber-like elasticity have a long chain and a poorly cross-linked structure. Elastic behaviour results from the entropy reduction associated with the twisting of the macromolecular chain from its most likely conformation. Nevertheless, the local movements of the chain segments must be limited to let polymer to return to its original shape, since the irreversible chains movement causes constant distortion of the material with each subsequent movement. Cross-linkages between the chains must be relatively few in order to facilitate high stretching without any breakage of the base bonds [8,9]. The glass transition temperatures (T_g) of biomedical polyurethanes range from about -50 to -80°C [4].

The main advantages of polyurethane links are following: easy fixing, lower transferred loads, aesthetic image, and the possibility of fluorine release [3]. Elastomeric ligatures are the main element supporting and maintaining wire arches in the channel of an orthodontic lock. Five most commonly used polymeric orthodontic ligatures produced by *Dentaurum*® were chosen for the tests. Three of them were of a chain type (denoted in the experiments as A, B, C); the next two were of a string type (D and E) – FIG. 1. The thickness of all chain ligatures was 1 mm, while the surface area in the thinnest place, for example, between the two "eyes", was 1 mm² for the A and B types and 1,4 mm² for the C ligature. For string ligatures, the values of the surface areas were 2.1 and 1.1 mm² for the D and E types, respectively.

Depending on the value and duration of the applied loading, two types of extrusion procedures are used in a clinical practice, so-called slow and fast or rapid. In the slow extrusion the total force applied to a one-root tooth should not exceed 30 G (approx. 0.3 N) and the total root displacement should be less than 1 mm per week – FIG. 2. For the fast extrusion, the load can be increased to 50 G (approx. 0.5 N). The procedure usually lasts for 4-8 weeks. Rapid extrusion is commonly used prior to further prosthetic treatment [3,10].

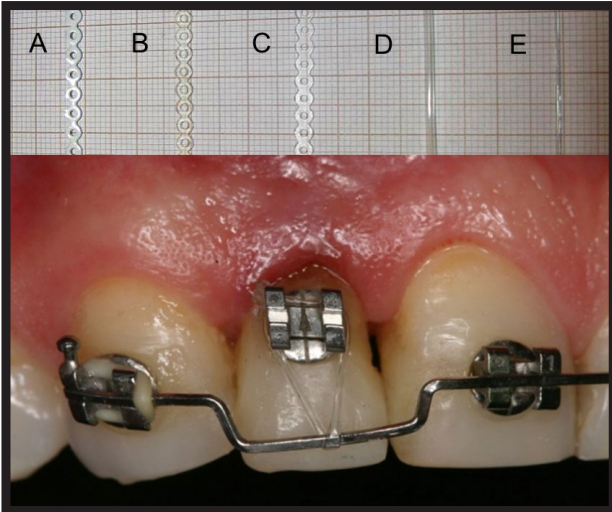


FIG. 1. Examples of the chain and string elastomeric ligature and their application in an orthodontic lock used in the extrusion treatment.

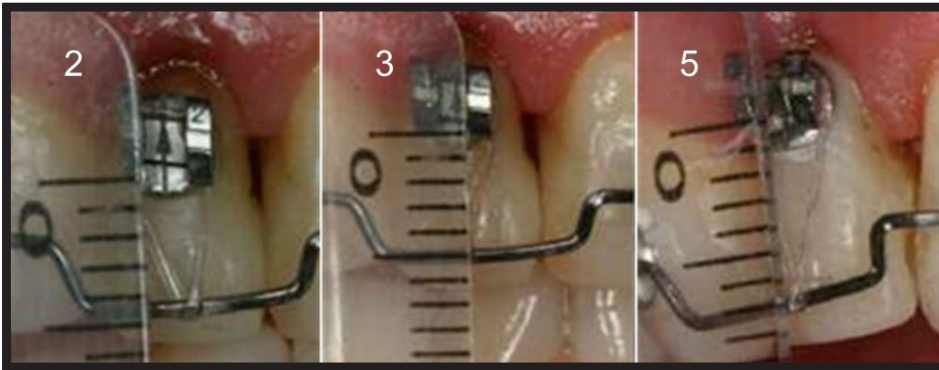


FIG. 2. Results of the orthodontic extrusion after 2, 3 and 5 weeks of the treatment.

Various rheological models were used to describe the stress relaxation behaviour of polyurethane ligatures: linear mechanical models, models based on the continuous distribution of relaxation time spectra, power-law models, exponential and cooperative models [11-13]. As the rheological properties of polyurethane elastomers are nonlinear, the paper presents the extrapolation fittings of the experimental curves in the power-law and exponential models.

The stress relaxation kinetics in polymers is often represented in terms of the stress dependent thermal activation, known also as the 'site model' theory [14,15]. The theory governs the dependencies of the relaxation times τ_{rel} upon the structural molecular changes, both conformational and chemical:

$$\tau_{rel} = \tau_0 \exp\left(-\frac{\Delta H}{kT}\right) \quad (1)$$

or

$$\tau_{rel} = \tau_0 \exp\left[\frac{(\Delta H - V\sigma)}{kT}\right], \quad (2)$$

where τ_0 is the basic atomic net thermal vibrations period, ΔH is the apparent activation energy of the process, T is the thermal energy, k is the Boltzmann constant, V is the elementary volume of the activation process, called also the 'free volume', and σ is the effective stress. The exponential law describes the stress relaxation in the following way:

$$\frac{d\sigma}{dt} \sim \exp\left(\frac{V\sigma}{kT}\right). \quad (3)$$

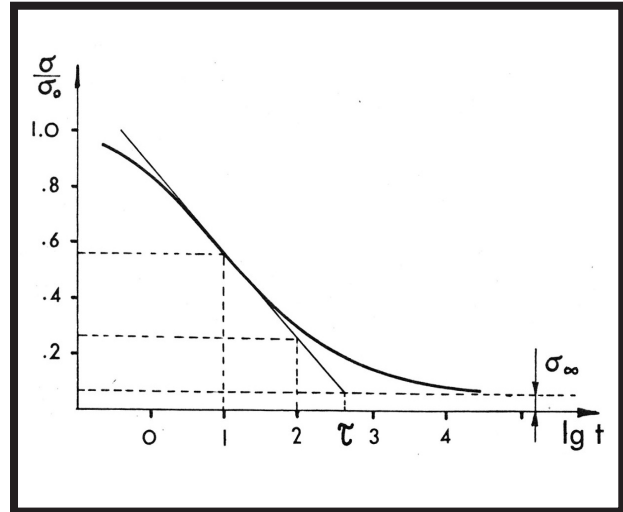


FIG. 3. Determination of the relaxation process parameters for the exponential models.

According to this rule, two types of the equations are commonly used for a wide range of polymeric materials [13]:

$$\frac{d\sigma}{dt} = -b \operatorname{sh}\left(\frac{\sigma}{F}\right) \quad (4)$$

and

$$\frac{d\sigma}{dt} = -b \left[\exp\left(\frac{\sigma}{F} - 1\right) \right], \quad (5)$$

where b and F are the parameters. The first model is known as Eyring's model, while the second stands for Kubat's model.

The parameter F represents the maximal slope (in the inflection point) of the relaxation curve plotted in the logarithmic time scale and the normalized stress (σ/σ_0) system of coordinates – FIG. 3. The parameter b is taken as $b = F/\tau$.

Power-law models generally undergo the rule $d\sigma/dt \sim \sigma^n$. The most commonly used model is known as Hook-Norton's law [14] which in terms of stress relaxation leads to the following relation:

$$\frac{d\sigma}{dt} = k \sigma^n, \quad (6)$$

where k and n are the parameters. The parameter k is proportional to the Young modulus of the polymer and is responsible for the stress relaxation course along the time axis, while the parameter n controls the slope of the relaxation curve. Based on the Hook-Norton's law, the American standards (ASTM) for the stress relaxation description suggest the following formula:

$$\sigma(t) = \frac{\sigma_0}{\left(1 + \frac{t}{b}\right)^a}, \quad (7)$$

with the a and b parameters. The ASTM stress relaxation representation corresponds to the Hook-Norton's law and the parameters $a \rightarrow 1/n$ and $1/b \rightarrow nk\sigma_0$. In that representation, for many thermoplastic polymers, the values of the a and b parameters take approximate values in the ranges (1.8-2.2) and (0.15-0.18), respectively.

Results and Discussions

Both the strength tests in the uniaxial stress state and the relaxation experiments for polyurethane ligatures were performed using the universal strength machine Instron 4465 – FIG. 4. The tensile tests were done for five samples in each group of ligatures. The medium values of the strength properties and the standard deviations for tensile stress for different polymeric ligatures in stress-strain test are shown in TABLE 1.

TABLE 1. Comparison of the strength properties of the examined polymeric ligatures in tensile tests.

Ligature type	Ultimate force [N]	Tensile stress [MPa]	SD	Maximal strain [%]
A	24	24.0	0.63	304
B	34	34.0	1.14	326
C	26	18.6	0.38	489
D	48	22.8	0.27	354
E	14	12.7	0.21	375



FIG. 4. A stand for tensile and relaxation tests of polyurethane ligatures.

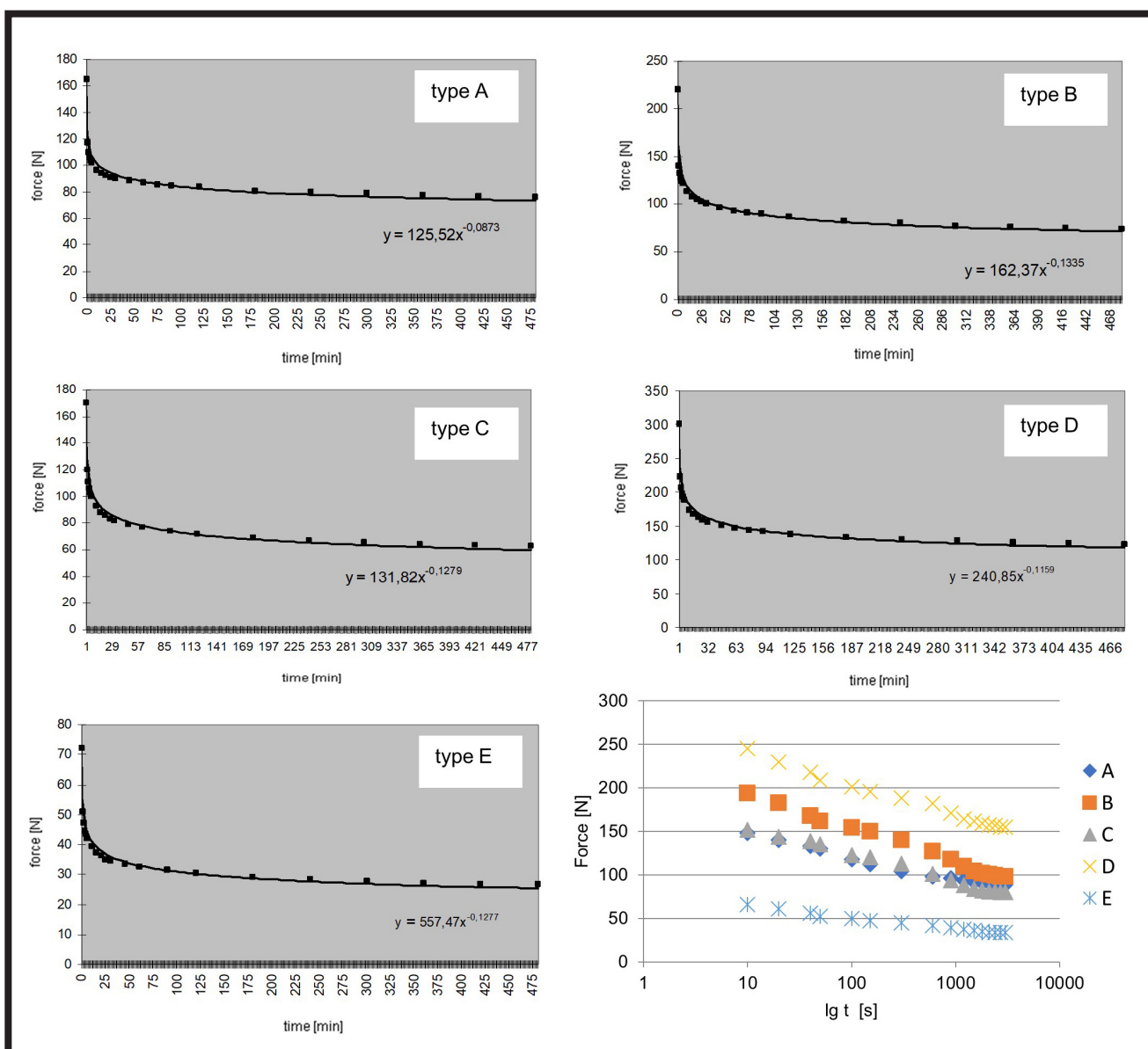


FIG. 5. Examples of the relaxation course for each group of the elastomeric ligatures.

Relaxation phenomenon seems to be a dominant feature in the time-dependent behaviour of those elements in orthodontic procedures, such as dentition corrections or teeth extrusions. Rheological properties of the elastomeric ligatures were examined in the relaxation tests in the uniaxial stress state for a set of 10 parallel arranged ligatures at room temperature and standard humidity.

FIG. 5 presents the examples of the relaxation course in each group of the polyurethane ligatures for approx. 8 hours of the experiments. TABLE 2 gives a set of the medium values of the relaxation percentage in all examined groups of ligatures after one week of the test. As the one-week stress relaxation tests are very time-consuming, three research trials were conducted in each group. Each experiment in a given research group was very comparable, especially with regard to the equilibrium relaxation determination, so no standard deviation analysis was done. Additionally, FIG. 5 presents a comparison of relaxation courses for all ligatures plotted in a logarithmic time scale. Regardless of the type of ligature, the basic relaxation time corresponding to the inflection point of the curve varies between 50 and 100 seconds, so that is why only the initial parts of the relaxation courses are presented.

TABLE 2. Comparison of the relaxation percentage in the examined polymeric ligatures after one week (168 hours).

Time [h]	Relaxation of ligature type [%]				
	A	B	C	D	E
168	34	22	24	28	24

The experiments proved that regardless of the type of ligature, the relaxation processes were relatively very fast. More than 50% of the initial force/stress disappeared after the first hour of relaxation. After one day, no more than 35% of the initial force/stress remained, while after a week it was approximately 25%. Starting from the second day, the daily force/stress decrease in the ligature ranged from 3 to less than 1%. The obtained regularities confirmed that the power-type relationship should only be used for low stress levels rheological processes. For all types of ligatures, the stress relaxation curves produced the similar exponent constant of the power-law model in the range -0.08 to -0.13. However, the proportional parameters were different, i.e. for chain ligatures the values varied in the 120-163 range and 240-560 for string ligatures, respectively.

The exponential models were excluded from further analyses as they were characterized with too fast final relaxation.

In clinical practice, both dentists and patients, during orthodontic extrusion report the uncontrolled decrease of the orthodontic force that leads to treatment failure. To simulate that undesirable phenomenon, the following experiment was carried out: five times, every hour, the displacement value (kinematic control) corresponding to the initial force of the relaxation force was reduced by 1 mm. The results of the experiments are presented in FIG. 6. To compensate for this disadvantage, dentists often use so-called 'secondary tightening' [16]. FIG. 7 presents the relaxation course in the elastomeric ligature in a two-steps relaxation process simulating the increase of orthodontic force in the secondary tightening. The first curve is an extrapolated plot of the D-type ligature relaxation for the initial force of 250 N. An hour later, the sample is restretched again to a ligature force of 200 N, which produces the relaxation given by curve no 2. The two-steps relaxation changes the value of the equilibrium stress. The asymptote of the first function is around 110 N, while the second is around 150 N, which provides the proper conditions for orthodontic extrusion.

The proper orthodontic extrusion assumes that the tooth should descend towards the occlusal line for about 0.15 mm per day. Correlations between stress-strain curves and stress relaxation characteristics estimate the therapeutic force that should be applied to the treated tooth in order to provide the extrusion phenomenon following the recommendations, i.e. at a rate of about 1 mm per week.

Regardless of the type of ligature, starting from the second day of the treatment comparable decrease values of both processes, i.e. the orthodontic extrusion force and the relaxation phenomenon, were registered. During the next two days, the decrease in force associated with the phenomenon of relaxation was approximately three times smaller than the decrease in force associated with the phenomenon of extrusion. Over the week, that difference was already of a smaller magnitude.

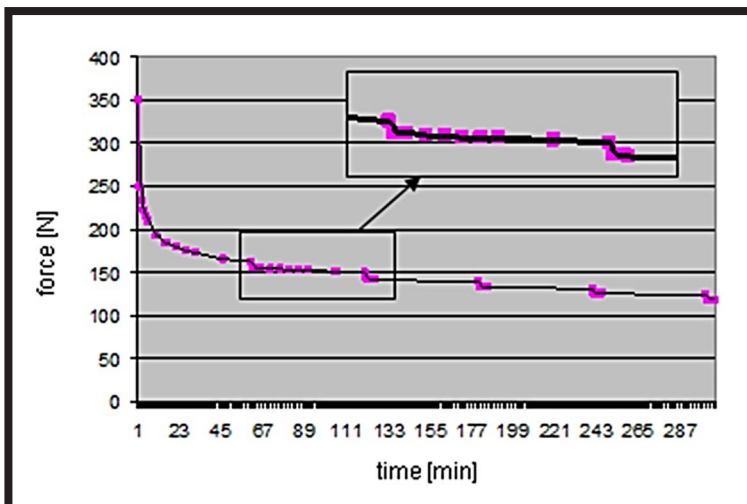


FIG. 6. The relaxation course in the type D elastomeric ligature in the simulated increase of tooth extrusion in orthodontic procedure.

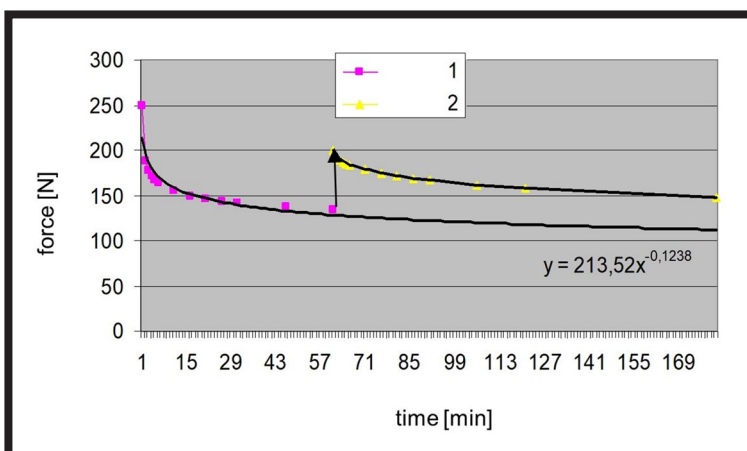


FIG. 7. The relaxation course in the type D elastomeric ligature in the two-steps process simulating the orthodontic force increase.

Conclusions

The most important conclusions from the research are as follows:

- the relationship between the strength and the elongation increments in biocompatible polyurethane ligatures is almost linear;
- the relaxation process runs most rapidly in the first phase of the phenomenon;
- a secondary increase in the ligature tension slows down the relaxation process and increases the asymptote value by about half of the difference between the primary and secondary tightening;
- after a day, the influence of the extrusion process on the decrease in strength begins to outweigh the influence of the relaxation process.

However, the exponential law which is based on the theory of rheological processes thermal activation is assumed in the literature to describe the best the relaxation behaviour of polymers. The results of relaxation experiments in elastomeric ligatures prove that, among various descriptions of that phenomenon, the power-law descriptions fit the best the time-dependent behaviour during orthodontic procedures. The power-law model gives the most intensive initial relaxation, which is characteristic for elastomeric ligatures.

Acknowledgements

Special thanks to Dr Anna Hille from Dental Clinic "Dentist" in Cracow for providing orthodontic ligatures for the tests and photos of the treatment progress.

ORCID iD

G. Milewski:

 <https://orcid.org/0000-0002-1854-0246>

References

- [1] Karłowska I. (ed.): An outline to modern orthodontics, PZWL, Warszawa, 2005.
- [2] Pawlaczyk K.: Forced orthodontic extrusion in multidisciplinary approach. Dent. Med. Probl. 43(4) (2006) 602-605.
- [3] Brantley W.A., Eliades T.: Orthodontic material – scientific and clinical aspects, Czelej, Lublin, 2003.
- [4] Zarow M., Vadini M., Chojacka-Brożek A., Szczekliak K., Milewski G., Biferi V., D'Arcangelo C., De Angelis F.: Effect of fiber posts on stress distribution of endodontically treated upper premolars: finite element analysis. Nanomaterials 10 (2020) 1-17.
- [5] Halimi A., Benyahia H., Doukkali A., Azeroual M.-F., Zaoui F.: A systematic review of force decay in orthodontic elastomeric power chains. International Orthodontics 10 (2012) 223-240.
- [6] Taloumis L.J., Smith T.M., Hondrum S.O., Lorton L.: Force decay and deformation of orthodontic elastomeric ligatures. American Journal of Orthodontics and Dentofacial Orthopedics 111 (1997) 1-11.
- [7] Lam T.V., Freer T.J., Brockhurst P.J., Podlich H.M.: Strength decay of orthodontic elastomeric ligatures. Journal of Orthodontics 29 (2002) 37-43.
- [8] Ferry J.D.: Viscoelastic properties of polymers. 3rd edition, 1980, John Wiley & Sons Inc., New York.
- [9] Brinson H.F., Brinson L.C.: Polymer Engineering Science and Viscoelasticity, 2015, Springer US, New York.
- [10] Milewski G., Hille A.: Experimental strength analysis of orthodontic extrusion of human anterior teeth. Acta of Bioengineering and Biomechanics 14 (2012) 15-21.
- [11] Cho K.S.: Viscoelasticity of polymers - theory and numerical algorithms, 2016, Springer Netherlands.
- [12] Christensen R.M.: Theory of viscoelasticity. 2nd edition, Dover Publications Inc., 2003, Mineola, New York.
- [13] Gutierrez-Lemini D.: Engineering viscoelasticity, 2014 Springer US, New York.
- [14] Ward J.M.: The mechanical properties of solid polymers, 1983, John Wiley & Sons Inc., New York.
- [15] Ward J.M., Sweeney J.: Mechanical properties of solid polymers. 3rd Edition, 2012, John Wiley & Sons Inc., New York.
- [16] Chang J.H., Hwang C.J., Kim K.H., Cha J.Y., Kim K.M., Yu H.S.: Effects of prestretch on stress relaxation and permanent deformation of orthodontic synthetic elastomeric chains. Korean J Orthod 48 (2018) 384-394.

POLY(SEBACIC ANHYDRIDE) MICROPARTICLES LOADED WITH CURCUMIN FOR PULMONARY PURPOSES

KONRAD KWIECIEŃ^{1*} , KATARZYNA RECZYŃSKA-KOLMAN¹ , DARIA NIEWOLIK² , KATARZYNA JASZCZ² , ELŻBIETA PAMUŁA¹ 

¹ AGH UNIVERSITY OF SCIENCE AND TECHNOLOGY, FACULTY OF MATERIALS SCIENCE AND CERAMICS, DEPARTMENT OF BIOMATERIALS AND COMPOSITES, A. MICKIEWICZ AV. 30, 30-059 KRAKÓW, POLAND

² SILESIAN UNIVERSITY OF TECHNOLOGY, DEPARTMENT OF PHYSICAL CHEMISTRY AND TECHNOLOGY OF POLYMERS, M. STRZODY STR. 9, 44-100 GLIWICE, POLAND

*E-MAIL: KKWIECIEN@AGH.EDU.PL

Abstract

Microparticles (MPs) made of fast biodegrading biomaterials, loaded with drugs, are considered a superior treatment method for pulmonary infections. One of the promising biomaterials for obtaining such a drug delivery system (DDS) is poly(sebacic anhydride) (PSA) due to its favourable degradation kinetics and mechanism.

In this paper, we present a study of manufacturing MPs from PSA loaded with curcumin (CU) for pulmonary purposes. MPs were manufactured by oil-in-water emulsification; their morphology and size distribution were evaluated using optical microscopy, while the encapsulation efficiency and drug loading were obtained by the fluorometric assay. The cytotoxicity of the MPs, both the empty ones and loaded with CU, was analysed by in vitro tests with BEAS-2B human lung epithelial cells. To this end, metabolic activity by AlamarBlue assay and fluorescent staining (DAPI/eosin) of the cells were performed.

The MPs produced were round, regular in shape with diameters in the range of 1-5 µm and of yellow colour originating from CU. The CU encapsulation efficiency ranged from 42% to 55% and decreased with a higher CU ratio. The drug loading ranged from 4% to 11% and increased at a higher CU ratio. Both empty and CU-loaded MPs did not show a cytotoxic effect at concentrations up to 10 µg/ml.

Keywords: poly(sebacic anhydride), curcumin, drug delivery system, pulmonary infections, polymeric microparticles

[Engineering of Biomaterials 162 (2021) 7-12]

doi:10.34821/eng.biomat.162.2021.7-12



Copyright © 2021 by the authors. Some rights reserved. Except otherwise noted, this work is licensed under <https://creativecommons.org/licenses/by/4.0>

Introduction

Chronic obstructive pulmonary disease (COPD) is a life-threatening lung dysfunction. It is believed to be the third major cause of mortality worldwide, which led to the death of 3.17 million people in 2015 (5% of all deaths) [1]. COPD patients suffer from acute exacerbations, half of which are of bacterial origin. Such events occur usually 1.5-2 times a year for patients with moderate to severe lung obstruction, and most of them require hospitalization [2]. Conventional therapy is based on oral or intravenous administration of antibiotics. The relatively small portion of the drug reaching the alveolar region of the lungs is the cause of using high doses that lead to multiple side effects mostly in the gastrointestinal system, liver, and kidneys [3]. Moreover, such treatment leads to gaining resistance to antibiotics by the bacteria and, in consequence, reduces the number of potent antibiotics to be used to treat future exacerbations [4].

Among the possible solutions, fast biodegrading polymeric microparticles (MPs) acting as drug carriers in the inhaled drug delivery systems (DDS) are considered a treatment method for pulmonary infections that could ensure the therapeutic effect without severe side effects and at lower risk of developing resistance to antibiotics [5]. Poly(sebacic anhydride) (PSA) is regarded as a suitable material for this purpose. It is superior to other degradable polymers, e.g. poly(lactide-co-glycolide) (PLGA), because of its fast degradation kinetics according to the surface erosion mechanism. PSA undergoes an almost complete decomposition after several days of incubation in an aqueous environment [6-8].

Drug carriers for pulmonary purposes delivered by inhalation have to meet several requirements. First, their diameter size should be optimal: too large carriers cannot reach the deep regions of the lungs, whereas too small carriers are removed while exhaling. The beneficial diameter size range in which a significant pulmonary deposition occurs is 1-5 µm [9]. However, the exact values are highly dependent on breath-holding while inhaling. For inhalation with and without breath-holding the maximum values were determined as 1.5-2.5 µm and 2.5-4 µm, respectively [10]. Another study confirmed that the MPs of such diameters have the highest alveolar deposition [11]. Moreover, the interactions between the carrier and the drug should support a high encapsulation efficiency. Physicochemical properties of the drug, the matrix and their compatibility strongly influence the drug loading capacity [12,13].

As it is not possible to eliminate antibiotics from COPD exacerbations treatment, it is important to reduce their doses without losing therapeutic effects. One approach to obtain that is to combine antibiotics with quorum sensing inhibitors (QSIs) [14,15]. Briefly, such substances inhibit bacterial activity and prevent bacteria from creating biofilm, making them more sensitive to antibiotics and the components of the patient's immune system [16]. Curcumin (CU) is an example of QSI, which is also a widely used colouring factor in the food industry. CU is also used in various studies for fluorescent labelling [17,18], enabling measurements of encapsulation efficiency by fluorometric assays. It was also shown that antibiotics used for pulmonary therapies (i.e. gentamycin, azithromycin) combined with curcumin show enhanced germicidal properties [19].

Therefore, in this study, we designed a novel inhalable DDS consisting of PSA MPs loaded with CU for the treatment of exacerbations in COPD patients. We characterised the PSA MPs properties and behaviour in contact with model human lung epithelial cells.

Materials and Methods

PSA was obtained by two-step melt polycondensation, as previously described [8]. Sebacic acid (10 g) was refluxed in acetic anhydride (1:10 w/v) under the nitrogen flow for 40 min. After this time, the excess of acetic anhydride and acetic acid formed in the reaction was removed under vacuum. The remaining diacyl derivative of sebacic acid (prepolymer) was heated at 150°C for 2 h with constant stirring under vacuum (0.1 mm Hg) and nitrogen. PSA in the form of a solid material was obtained with a yield of more than 90%. The obtained polymer was stored in a freezer. The thermal properties of the polymer were investigated using the 822° DSC Mettler Toledo differential scanning calorimeter. The sample was tested in a temperature range of -70°C to 250°C at a heating rate of 10°C/min. The structure of PSA was studied by the ¹H and ¹³C NMR spectroscopy (Varian UNITY/INOVA spectrometer (300 MHz)) ¹H NMR (CDCl₃, ppm) δ: 2.40 - 2.50 (m, 4H, -CH₂C(O)OC(O)-), 2.22 (s, 6H, CH₃C(O)OC(O)-), 1.55 - 1.74 (m, 4H, -CH₂CH₂C(O)OC(O)-), 1.22 - 1.44 (m, 8H, -CH₂-). ¹³C NMR (75 MHz, CDCl₃, ppm) δ: 169.53 (C=O, anhydride), 35.18 (-CH₂C(O)OC(O)-), 28.80 (-CH₂CH₂C(O)OC(O)-), 24.10 (-CH₂-).

The molecular weight (M_w) of PSA was determined in methylene chloride by gel-permeation chromatography (GPC) using Agilent Technologies Infinity 1260 chromatograph that was equipped with a refractive index detector and calibrated with polystyrene standards. The sample was pre-filtered prior to analysis. The evaluation of M_w by the ¹H NMR analysis was calculated on the basis of dependence shown in eq. 1:

$$M_w = n_{SA} \cdot M_{SA} + M_{end\ groups} \quad (1)$$

where: M_w - molecular weight, n_{SA} - number of repeating unit of PSA, M_{SA} - molar mass of repeating unit of PSA, $M_{end\ groups}$ - molar mass of end groups in polyanhydride equal to 102 g/mol.

The n_{SA} parameter was calculated from the ¹H NMR spectra as the intensity ratio between PSA protons and end groups protons as in eq. 2:

$$n_{SA} = \frac{I_{[1H]SA}}{I_{[1H]end\ groups}} \quad (2)$$

where: $I_{[1H]SA}$ - intensity of one PSA proton, $I_{[1H]end\ groups}$ - intensity of one proton of end groups.

MPs were manufactured using solid-in-oil-in-water emulsification (S/O/W). As a solid phase (S) different amounts of CU (Sigma-Aldrich) – 3 mg, 6 mg, and 12 mg per batch (5, 10, and 20 mg / 100 mg of PSA, respectively, equal to CU:PSA ratio of 1:20, 1:10 and 1:5, respectively), were used. As an oil phase (O), a PSA solution in dichloromethane (DCM) (Chemland) – 20 mg/ml was prepared. As a water phase acted the (W) poly(vinyl alcohol) (PVA) (Mowiol® 4-88, M_w = 31 kDa, Sigma-Aldrich) solution in ultra-high quality water (UHQ-water) – 80 mg/ml. Before the process, all the O and W phases were cooled in ice. The CU portions were dissolved in 3 ml of the PSA solution in DCM using an ultrasound probe (1 min, amplitude 40%, pulsation workpause 10 s – 5 s; SONICS Vibra cell). The 20 ml of the W phase was placed on the magnetic stirrer (JEIO TECH Multichannel stirrer) at 1500 rpm. Then, 3 ml of the O phase was poured into the W phase with constant stirring. The organic solvent was being evaporated for 4.5 h under constant magnetic stirring. The suspension of MPs was then collected and centrifuged (MPW-351R) at 15000 rpm for 10 min to remove the PVA excess from the MPs; the process was repeated 3 times. The water after the first 2 centrifugations was collected for encapsulation efficiency studies.

Then, the MPs were freeze-dried for 24 h (Martin Christ Alpha 1-2 LDplus) and stored at -20°C.

The morphology of the MPs was evaluated using an optical microscope (ZEISS Axiovert 40 CFL), and the diameter of the MPs was measured using ImageJ software ($n = 1000$).

The encapsulation efficiency of CU was determined in the supernatant after the MPs centrifugation using a fluorometric assay. The samples of the supernatant were diluted with dimethyl sulfoxide (DMSO) (POCH S.A.) in a volumetric ratio of 1:10 to dissolve residual CU. CU in known concentrations (0-100 µg/ml, step 10 µg/ml) was dissolved in the same mixture water:DMSO (1:10) for the preparation of the calibration curve. The linear relationship was evaluated in the range 0-20 µg/ml CU.

The samples of both calibrations and supernatants diluted in DMSO were placed in a black 96-well TCPS plate (100 µl/well, $n = 3$ for each sample). Measurements at excitation wavelength 485-412 nm and emission wavelength 590-510 nm were made using the plate reader (FluoStar OMEGA, BMG LabTech).

The encapsulation efficiency was determined as:

$$Encapsulation\ efficiency = \frac{encapsulated\ CU}{initial\ CU\ addition} \cdot 100\% \quad (3)$$

and the drug loading was determined as:

$$Drug\ loading = \frac{encapsulated\ CU}{MP\ mass} \cdot 100\% \quad (4)$$

BEAS-2B human lung epithelial cells (ATCC, CRL-9609™) were used to evaluate the biological properties of the developed MPs system. The cells were cultured in cell culture flasks in Dulbecco's modified Eagle's medium (DMEM) with 10% volume of fetal bovine serum (FBS) and 1% mixture of penicillin (10,000 U/ml) and streptomycin (10 mg/ml) (all chemicals from PAN Biotech). Before the experiment, the cells were seeded in a 96-well TCPS plate (10 000 cells/well in 100 µl medium) and incubated for 24 h at 37°C and 5% CO₂. Then, the medium was replaced with the suspension of empty and CU-loaded MPs (CU:PSA equal to 1:10) at different concentrations from 0 to 1000 µg/ml.

To test cell metabolic activity, an AlamarBlue assay (resazurin-based, Sigma-Aldrich) was performed. The MPs were sterilized by 40-minute exposure to UV radiation. After the 24 h incubation of the cells with MPs, the suspensions were removed and the cultured cells were washed with Dulbecco's Phosphate Buffer Saline (DPBS) (PAN Biotech). The resazurin reduction based viability assay (AlamarBlue, Sigma-Aldrich) was conducted by filling each well with 150 µl of 10% AlamarBlue solution in DMEM and 3 h incubation at 37°C. The fluorescence was then measured using the fluorometer (FluoStar OMEGA, BMG LabTech) at the excitation wavelength 544 nm and the emission wavelength 590 nm. The relative reduction of resazurin was evaluated using the equation:

$$RR = \frac{F_{sample} - F_0}{F_{100} - F_0} \quad (5)$$

where: RR - resazurin reduction, F_{sample} - fluorescence measured for the sample, F_0 - fluorescence measured for the DMEM-AlamarBlue mixture incubated in empty wells (0% relative resazurin reduction), F_{100} - fluorescence measured for DMEM-AlamarBlue mixture completely reduced in an autoclave (100% relative resazurin reduction). The statistical significance of the obtained differences was evaluated with ANOVA and the *post hoc* Tukey HSD test.

The 4',6-Diamidino-2-Phenylindole (DAPI, Sigma Aldrich) and eosin (Thermo Scientific) fluorescence staining was performed to evaluate the cell morphology. Before staining, the MPs suspension was removed from the wells, the cells were washed with DPBS with the addition of Ca/Mg ions (PAN Biotech), and the cells were fixed with 4% paraformaldehyde (Sigma-Aldrich) for 15 min. The cells were then washed 2 times with DPBS-Ca/Mg, incubated in the 0.1% Triton X solution (Sigma Aldrich), and again washed 2 times with DPBS-Ca/Mg. The preserved cells were incubated for 5 min in the eosin solution (0.5 % (w/v) in acidified ethanol, Sigma Aldrich), washed 5 times with DPBS-Ca/Mg and incubated in the DAPI solution for 15 min, and washed 3 times. Finally, the observations were made on a fluorescent microscope (ZEISS Axiovert 40 CFL) with ZEISS HXP 120 C metal halide illuminator.

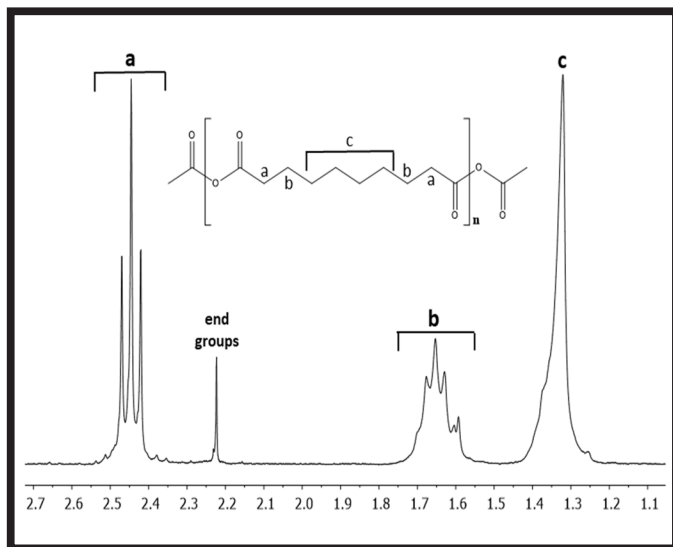


FIG. 2. ^1H NMR spectra of PSA.

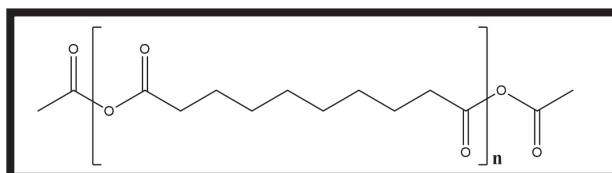


FIG. 1. Chemical structure of PSA.

Results and Discussions

Poly(sebacic acid) structure and properties

Poly(sebacic acid) (PSA) was obtained by melt polycondensation of sebacic acid with the use of acetic anhydride. The structural formula of PSA is presented in FIG. 1.

The obtained polymer was a solid crystalline material, with a melting temperature $T_m = 82^\circ\text{C}$. The relative crystallinity estimated by dividing the determined heat of fusion of PSA ($\Delta H_m = -94.6 \text{ J/g}$) by theoretical value (-115 J/g) was equal to 80%. The polymer was found to be soluble in chlorinated and partially in aromatic solvents, but insoluble in water, ethanol, acetone, diethyl ether, hexane, THF and DMSO. To determine the structure of PSA, the ^1H NMR spectra (FIG. 2) and ^{13}C NMR spectra were made. The successful synthesis of polyanhydride was confirmed by the anhydride bond formation. The presence of the signal at $\delta = 169.53 \text{ ppm}$ (in the ^{13}C NMR spectrum), assigned to carbonyl carbon atoms in anhydride, and the signal at $\delta = 2.40\text{--}2.50 \text{ ppm}$ (in ^1H NMR spectrum), assigned to methylene protons close to anhydride groups, confirmed the formation of anhydride bonds.

The molecular weight of PSA was calculated from ^1H NMR and determined by GPC. The molecular weight calculated from ^1H NMR was approximately 10,000 Da, which corresponded to a polymer consisting of ca. 50 repeating units, whereas the one determined by GPC was 10800 Da. It indicates a good correlation between the obtained molecular weights.

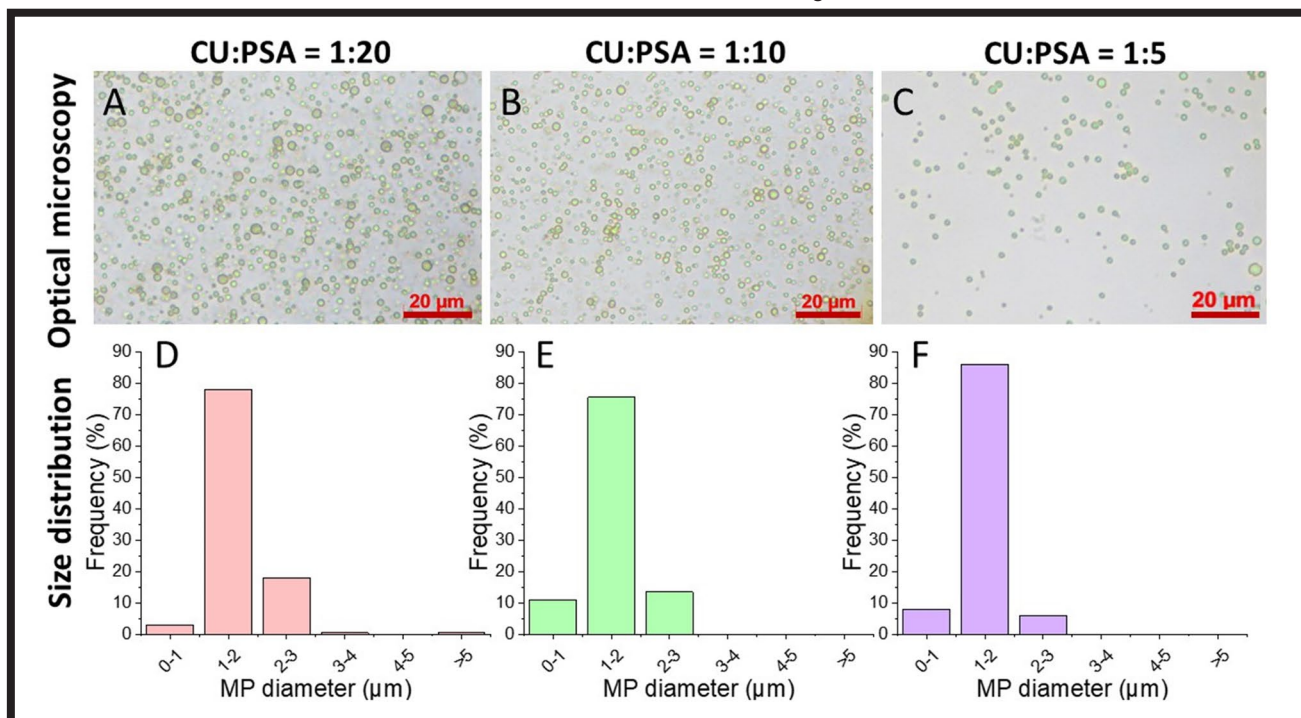


FIG. 3. Morphology (A, B, C) and size distribution (D, E, F) of PSA microparticles with different concentrations of curcumin to PSA (weight ratio): 1:20 (A, D), 1:10 (B, E) and 1:5 (C, F) – pictures from the optical microscope and histograms of diameter size distributions.

Microparticle morphology and size

The manufactured MPs were spherical in shape and yellow from the encapsulated CU (FIG. 3 A-C). In all the cases, the majority of the MPs had diameters in the range of 1-2 μm . The number of MPs with diameters exceeding 5 μm was negligible. There were some MPs with the diameter smaller than 1 μm (FIG. 3 D-F). Yet, in each case, more than 90% of the MPs were in the appropriate size for administration via inhalation [9]. However, to obtain the best pulmonary deposition, the MPs could have slightly larger diameters to fit more to the range of 1.5-2.5 μm [10]. The median size gradually decreased with an increasing CU:PSA weight ratio (median: 1.53 μm , 1.48 μm , and 1.43 μm for CU:PSA equal to 1:20, 1:10 and 1:5, respectively).

Encapsulation efficiency and drug loading

The encapsulation efficiency and resulting MPs loading was evaluated for all the batches. For the 1:20 and 1:10 CU:PSA ratio, we obtained the encapsulation efficacies without significant differences ($\alpha = 0.05$) – $54.6 \pm 1.0\%$ and $55.0 \pm 2.6\%$, respectively. At the 1:5 ratio, the efficiency decreased significantly ($p < 0.001$) to $42.8 \pm 0.7\%$ (FIG. 4A). However, the drug loading increased significantly ($p < 0.001$) at each subsequent higher CU ratio – $4.5 \pm 0.1\%$, $7.9 \pm 0.4\%$, and $11.0 \pm 0.2\%$ for 1:20, 1:10 and 1:5 CU:PSA ratio, respectively (FIG. 4B). Although the process was less efficient at a higher CU ratio, the final drug loading was much higher. The encapsulation efficiency was satisfactory but not very high, so future work may focus on improving that value. In the other studies, for similar MPs made out of PLGA for different biomedical purposes, the encapsulation efficiencies were higher, e.g. around 67% for lipid-PLGA hybrid MPs [20] and up to around 95% for PLGA MPs with electrospray droplet formulation [21]. On the other hand, the most important value is the drug loading, and manufacturing the MPs that consist of the drug in 11% mass is a promising result that confirms a good CU-PSA compatibility. For comparison, in [20] the drug loading was evaluated as $1.85 \pm 0.19\%$. All of the MPs glowed intensively in green colour under a fluorescence microscope (FIG. 4C), indicating that the CU was effectively and uniformly encapsulated within the MPs.

In vitro tests of microparticles

The BEAS-2B cells were cultured for 24 h and then the MPs (empty or CU-loaded, obtained at CU:PSA ratio 1:10) suspensions (concentrations: 0.1, 1, 5, 10, 50, 100, 500, and 1000 $\mu\text{g}/\text{ml}$ DMEM) were added to the wells. To evaluate the viability of the cells incubated in contact with the MPs for 24 h, the metabolic test AlamarBlue was performed on both the empty MPs and CU-loaded MPs. The fluorescent staining by DAPI/eosin was performed to assess the cell morphology.

AlamarBlue tests did not show a cytotoxic effect up to 10 $\mu\text{g}/\text{ml}$ for both empty (FIG. 5A) and CU-loaded MPs (FIG. 5B). Above this concentration (up to 100 $\mu\text{g}/\text{ml}$), a gradual decrease in the cell viability was observed. The reduction of resazurin decreased by 23.8% for 50 $\mu\text{g}/\text{ml}$ and by 35.5% for 100 $\mu\text{g}/\text{ml}$ for the empty MPs suspensions, and by 22.4% for 50 $\mu\text{g}/\text{ml}$ and by 36.1% for 100 $\mu\text{g}/\text{ml}$, as compared to the control. For the highest concentrations of MPs (500 and 1000 $\mu\text{g}/\text{ml}$) the viability decreased rapidly by 90.3% for 500 $\mu\text{g}/\text{ml}$ and by 98.4% for 1000 $\mu\text{g}/\text{ml}$ (empty MPs), and by 70.3% for 500 $\mu\text{g}/\text{ml}$ and by 84.8% for 1000 $\mu\text{g}/\text{ml}$. These results were consistent with the DAPI/eosin staining. The cells cultured in contact with MPs looked similar in each well with a low concentration of MPs suspension. For 50 $\mu\text{g}/\text{ml}$ and higher concentrations, a significant amount of the stained MPs residue was visible in each well, with a decreasing number of cells. The cells nuclei were DAPI stained in all cases. The cytoplasm was stained with eosin; however, it was properly stained only up to the 50 $\mu\text{g}/\text{ml}$ MPs concentration. For concentrations of 100 $\mu\text{g}/\text{ml}$ and 1000 $\mu\text{g}/\text{ml}$, the signal from the MPs residues was too strong. We chose DAPI (blue staining of cell nuclei) and eosin (red staining of the cytoskeleton) to avoid overlapping of green colour from the MPs (FIG. 4C). However, this was not sufficient, as the residues of degraded MPs, which were not removed during washing, absorbed eosin, resulting in a very intense red glow, much brighter than the cytoplasm of the cells stained by eosin. Zhang et al. [22] tested a PSA-based polymer, synthesized with poly(ethylene glycol), nanoparticles *in vitro* in contact with L929 and MCF-7 cell lines and obtained no cytotoxicity up to 220 $\mu\text{g}/\text{ml}$. The cytotoxic effect observed in this study at lower concentrations could result from the high sensitivity of BEAS-2B cells.

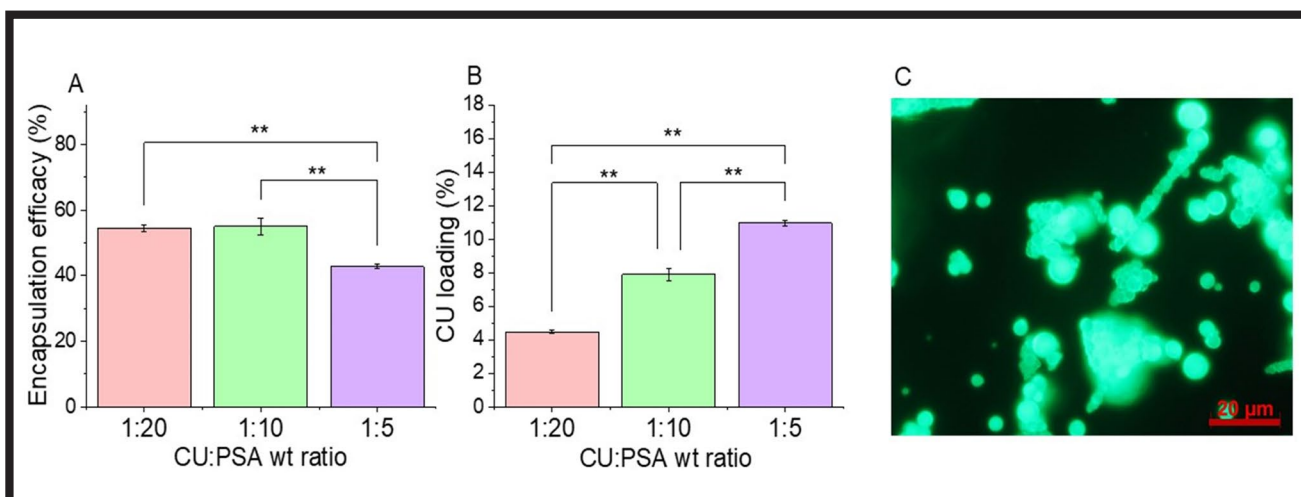


FIG. 4. Encapsulation efficiency (A), CU loading in the PSA MPs (B), and a picture from the fluorescent microscope (MPs obtained with CU:PSA ratio of 1:10) (C); * - $p < 0.01$, ** - $p < 0.001$ – the significance levels, according to ANOVA and post hoc Tukey HSD test.

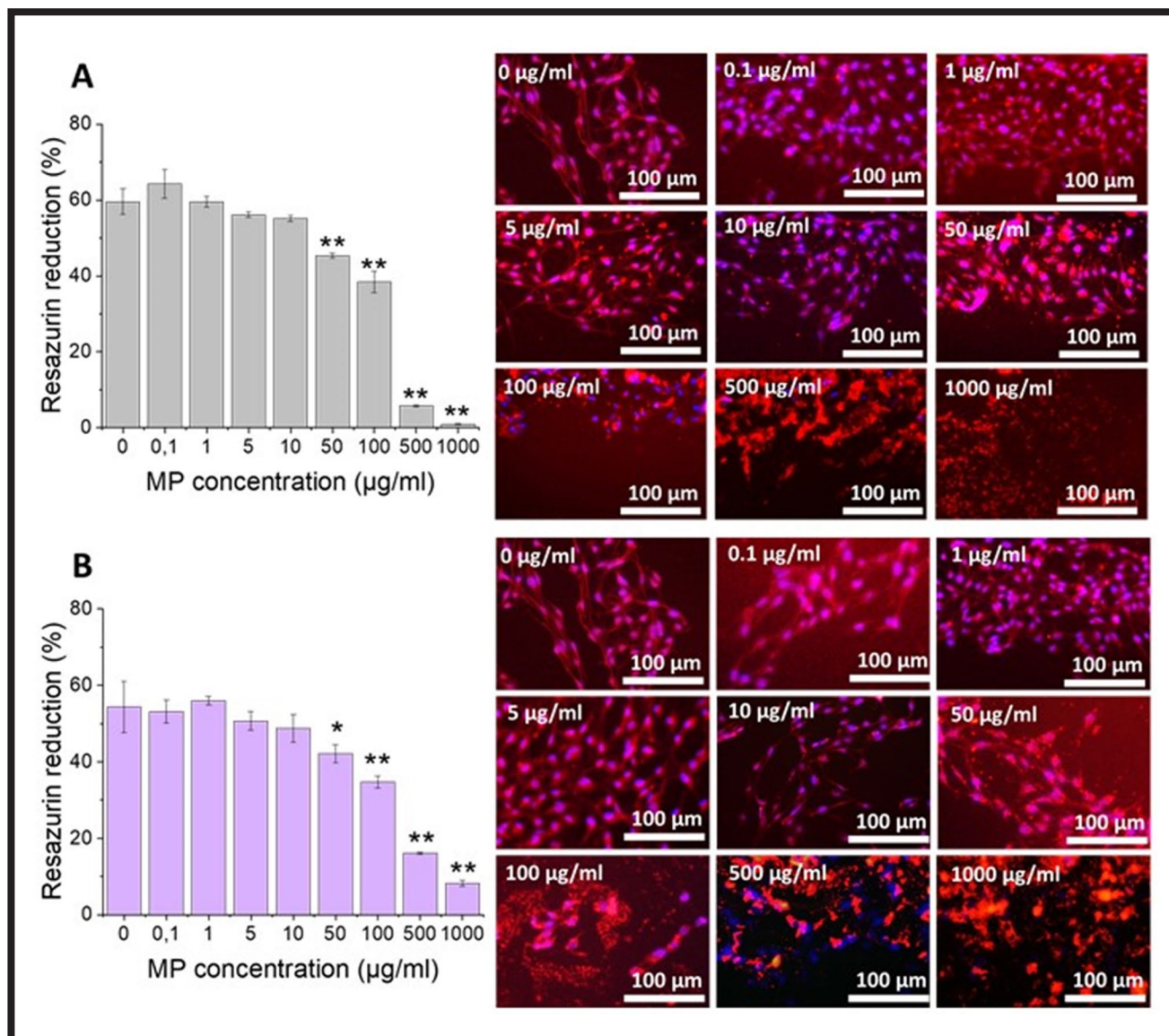


FIG. 5. Cytotoxicity test results – AlamarBlue (left) and DAPI/eosin fluorescent staining (right). A – empty MPs, B – CU-loaded MPs; * - $p < 0.01$, ** - $p < 0.001$ – significance levels, according to ANOVA and the post hoc Tukey HSD test.

The AlamarBlue results indicated that CU-loaded MPs were less cytotoxic than the empty ones: the difference in viability at 50 µg/ml was less significant for the CU-loaded MPs. However, the AlamarBlue is a fluorescent test. Therefore, there is a possibility that the evaluated resazurin reductions for the CU-loaded MPs overlapped with the signal of the MPs residue unwashed from the well. Such an effect is possible. As it was previously proved, pure CU influences the BEAS-2B cells negatively, and the influence decreases while the CU is encapsulated within the liposomes [23]. On the other hand, overlapping should be observed at a significant level only for the wells where the relatively high concentrations of MPs were applied (i.e. 500, 1000 µg/ml). At these concentrations, the pictures from the fluorescent microscope showed a significant amount of MPs residues that could influence the measurements. Below these concentrations, the significant overlapping is much less probable. However, this conclusion should be confirmed in the future by evaluating the background from the CU-loaded MPs residue at the analysed concentrations.

Conclusions

This work aimed to manufacture the cytocompatible CU-loaded PSA MPs with the 1-5 µm diameter size f, the narrow size distribution, and the sufficient CU loading. Three batches of the MPs were prepared using different ratios of CU to PSA: 1:20, 1:10, and 1:5. In all the samples, more than 90% of the MPs had diameters in the range of 1-3 µm, meeting the size and uniform distribution conditions for administration via inhalation. Additionally, all the MPs were spherical and of yellow colouration resulting from the CU encapsulation.

The encapsulation efficiency was satisfactory in the range of 42-55% and decreased with a higher CU:PSA ratio. On the other hand, the CU loading increased at a higher CU ratio from $4.5 \pm 0.1\%$ to exquisite $11.0 \pm 0.2\%$.

The cytocompatibility tests did not show a toxic effect at the low concentrations of MPs in the suspension (up to 10 µg/ml). Above that concentration, the viability of the cells gradually decreased for both the empty and CU-loaded MPs. However, the cells in contact with CU-loaded MPs showed a slightly lower decrease in their metabolic activity, indicating that the presence of CU decreased the system toxicity.

To sum up, it was possible to manufacture the MPs from PSA in the proper sizes for pulmonary administration that are loaded with CU in a sufficient ratio. Such MPs appear to be safe for human lung epithelial cells (BEAS/2B) up to 10 µg/ml. The surface of a single well was 0.33 cm² which is approximately 10⁶ times smaller than the surface area of the human lung, indicating the cytocompatible limit of the MPs to be administrated at around 30 g. Moreover, the limit of MPs concentration per surface unit should be higher *in vivo*, as the cells in the tissue are densely packed. Therefore, the cytotoxicity evaluated in this study should not be a limitation for pulmonary purposes. However, this is only an estimation. Without the aerodynamics study of the MPs using a cascade impactor, it is not possible to determine the exact amount of the MPs that would reach the alveolar region. The example of such a study [24] showed that the alveolar deposition of an inhalable aerosol with particles in the diameter range of 4.70–5 µm could be estimated at around 7.7–11.5%. Therefore, future studies will focus on the following methodological aspects: 1) determining the fluorescent background of the degraded MPs residue in the AlamarBlue test, 2) choosing another cell visualisation method to prove the superior cytocompatibility of CU-loaded MPs to the empty ones, and

3) eliminating the signal overlapping from the MPs during fluorescent microscopic observations, as by eosin staining. Moreover, the future work will focus on the further increase of the CU loading within the PSA MPs or MPs obtained from other polyanhydrides and the co-encapsulation of CU and antibiotics in one formulation, accompanied by evaluating its germicidal properties.

Acknowledgements

This study was supported by the National Science Center, Poland (project No. 2019/35/B/ST5/01103) and by the Program "Excellence Initiative – Research University" for the AGH University of Science and Technology.

ORCID iDs

K. Kwiecień: <https://orcid.org/0000-0002-9504-1205>
 K. Reczyńska-Kolman: <https://orcid.org/0000-0002-5266-9131>
 D. Niewolik: <https://orcid.org/0000-0003-2472-3943>
 K. Jaszcz: <https://orcid.org/0000-0003-4883-8278>
 E. Pamuła: <https://orcid.org/0000-0002-0464-6189>

References

- [1] J.B. Soriano, A.A. Abajobir, K.H. Abate, et al.: Global, regional, and national deaths, prevalence, disability-adjusted life years, and years lived with disability for chronic obstructive pulmonary disease and asthma, 1990–2015: a systematic analysis for the Global Burden of Disease Study 2015. *Lancet Respir Med* 5(9) (2017) 691–706, doi: 10.1016/S2213-2600(17)30293-X.
- [2] C.F. Vogelmeier, G.J. Criner, F.J. Martinez, et al.: Global Strategy for the Diagnosis, Management, and Prevention of Chronic Obstructive Lung Disease 2017 Report. GOLD Executive Summary. *Am J Respir Crit Care Med* 195(5) (2017) 557–582, doi: 10.1164/rccm.201701-0218
- [3] J. Marchant: When antibiotics turn toxic. *Nature* 555(7697) (2018) 431–433, doi: 10.1038/d41586-018-03267-5.
- [4] R. Hershberg: Antibiotic-Independent Adaptive Effects of Antibiotic Resistance Mutations. *Trends in Genetics* 33(8) (2017) 521–528, doi: 10.1016/j.tig.2017.05.003.
- [5] A.K. Thakur, D.K. Chellappan, K. Dua, M. Mehta, S. Satija, I. Singh: Patented therapeutic drug delivery strategies for targeting pulmonary diseases. *Expert Opinion on Therapeutic Patents* 30(5) (2020) 375–387, doi: 10.1080/13543776.2020.1741547.
- [6] J. Fu, C. Wu: Laser light scattering study of the degradation of poly(sebacic anhydride) nanoparticles. *Journal of Polymer Science Part B: Polymer Physics* 39(6) (2001) 703–708, doi: 10.1002/1099-0488(20010315)39:6<703::AID-POLB1044>3.0.CO;2-B.
- [7] Z. Deng, A. Schweigerdt, A. Norow, K. Lienkamp: Degradation of Polymer Films on Surfaces: A Model Study with Poly(sebacic anhydride). *Macromolecular Chemistry and Physics* 220(15) (2019) 1900121, doi: 10.1002/macp.201900121.
- [8] K. Jaszcz: Synthesis and Characterization of New Functional Poly(ester-anhydride)s Based on Succinic and Sebacic Acids. *Macromol. Symp.* 254(1) (2007) 109–116, doi: 10.1002/masy.200750817.
- [9] M. Paranjpe, C.C. Müller-Goymann: Nanoparticle-Mediated Pulmonary Drug Delivery: A Review. *International Journal of Molecular Sciences* 15(4) (2014) Art. 4, doi: 10.3390/ijms15045852.
- [10] P.R. Byron: Prediction of Drug Residence Times in Regions of the Human Respiratory Tract Following Aerosol Inhalation. *Journal of Pharmaceutical Sciences* 75(5) (1986) 433–438, doi: 10.1002/jps.2600750502.
- [11] J. Heyder, J. Gebhart, G. Rudolf, C.F. Schiller, W. Stahlhofen: Deposition of Particles in the Human Respiratory Tract in the Size Range 0.005–15 µm. *Journal of Aerosol Science* 17(5) (1986) 811–825.
- [12] S.R. Shah, A.M. Henslee, P.P. Spicer, et al.: Effects of Antibiotic Physicochemical Properties on Their Release Kinetics from Biodegradable Polymer Microparticles. *Pharm Res* 31(12) (2014) 3379–3389, doi: 10.1007/s11095-014-1427-y.
- [13] Z. Huang, S.N. Kłodzińska, F. Wan, H.M. Nielsen: Nanoparticle-mediated pulmonary drug delivery: state of the art towards efficient treatment of recalcitrant respiratory tract bacterial infections. *Drug Deliv. and Transl. Res.* 11(4) (2021) 1634–1654, doi: 10.1007/s13346-021-00954-1.
- [14] V.C. Kalia: Quorum sensing inhibitors: An overview. *Bio-technology Advances* 31(2) (2013) 224–245, doi: 10.1016/j.biotechadv.2012.10.004.
- [15] M. Whiteley, S.P. Diggle, E.P. Greenberg: Progress in and promise of bacterial quorum sensing research. *Nature* 551(7680) (2017) 313–320, doi: 10.1038/nature24624.
- [16] T. Defoirdt, G. Brackman, T. Coenye: Quorum sensing inhibitors: how strong is the evidence? *Trends in Microbiology* 21(12) (2013) 619–624, doi: 10.1016/j.tim.2013.09.006.
- [17] E. Akbari, O. Akhavan, S. Hatamie, R. Rahighi: Curcumin as a green fluorescent label to revive the fluorescence property of functionalized graphene oxide nanosheets. *Journal of Drug Delivery Science and Technology* 45 (2018) 422–427, doi: 10.1016/j.jddst.2018.04.010.
- [18] A. Kumar, L. Li, A. Chaturvedi, J. Brzostowski, et al.: Two-photon fluorescence properties of curcumin as a biocompatible marker for confocal imaging. *Appl. Phys. Lett.* 100(20) (2012) 203701, doi: 10.1063/1.4717753.
- [19] S. Bahari, H. Zeighami, H. Mirshahabi, S. Roudashti, F. Haghi: Inhibition of *Pseudomonas aeruginosa* quorum sensing by subinhibitory concentrations of curcumin with gentamicin and azithromycin. *Journal of Global Antimicrobial Resistance* 10 (2017) 21–28, doi: 10.1016/j.jgar.2017.03.006.
- [20] P.-C. Li, S.-C. Chen, Y.-J. Hsueh, et al.: Gelatin scaffold with multifunctional curcumin-loaded lipid-PLGA hybrid microparticles for regenerating corneal endothelium. *Materials Science and Engineering: C* 120 (2021) 111753, doi: 10.1016/j.msec.2020.111753.
- [21] S. Yuan, F. Lei, Z. Liu, Q. Tong, T. Si, R.X. Xu: Coaxial Electrospray of Curcumin-Loaded Microparticles for Sustained Drug Release. *PLOS ONE* 10(7) (2015) e0132609, doi: 10.1371/journal.pone.0132609.
- [22] J. Zhang, Y. Liang, N. Li, et al.: Poly(ether-ester anhydride)-based amphiphilic block copolymer nanoparticle as delivery devices for paclitaxel. *Micro Nano Lett.* 7(2) (2012) 183, doi: 10.1049/mnl.2011.0580.
- [23] T. Zhang, Y. Chen, Y. Ge, Y. Hu, M. Li, Y. Jin: Inhalation treatment of primary lung cancer using liposomal curcumin dry powder inhalers. *Acta Pharmaceutica Sinica B* 8(3) (2018) 440–448, doi: 10.1016/j.apsb.2018.03.004.
- [24] J. Fiegel, L. Garcia-Contreras, M. Thomas, et al.: Preparation and *In Vivo* Evaluation of a Dry Powder for Inhalation of Capreomycin. *Pharm Res* 25(4) (2008) 805–811, doi: 10.1007/s11095-007-9381-6.

PREPARATION AND PRELIMINARY *IN VIVO* STUDIES OF RESORBABLE POLYMER MODIFIED WITH ALLOGENIC BONE CHIPS FOR GUIDED BONE REGENERATION AND ORTHOPEDIC IMPLANTS

BARBARA SZARANIEC^{1*} , TOMASZ SZPONDER² ,
KAROL GRYN¹ , MACIEJ AMBROZIAK³ , GRZEGORZ
GUT⁴ , ŁUKASZ KOPERSKI⁴ , JAN CHŁOPEK^{1†} 

¹ AGH UNIVERSITY OF SCIENCE AND TECHNOLOGY,
FACULTY OF MATERIALS SCIENCE AND CERAMICS,
DEPARTMENT OF BIOMATERIALS AND COMPOSITES,
AL. MICKIEWICZA 30, 30-059 KRAKÓW, POLAND

² UNIVERSITY OF LIFE SCIENCES IN LUBLIN,
FACULTY OF VETERINARY MEDICINE,
DEPARTMENT AND CLINIC OF VETERINARY SURGERY,
UL. GŁĘBOKA 30, 20-612 LUBLIN, POLAND

³ CHAIR AND CLINIC OF ORTHOPAEDICS AND TRAUMATOLOGY,
MEDICAL UNIVERSITY OF WARSAW,
UL. W. LINDLEYA 4, 02-005 WARSAW, POLAND

⁴ DEPARTMENT OF TRANSPLANTOLOGY AND CENTRAL
TISSUE BANK, MEDICAL UNIVERSITY OF WARSAW,
UL. CHALUBINSKIEGO 5, 02-004 WARSAW, POLAND

*E-MAIL: SZARAN@AGH.EDU.PL

† THE AUTHOR RECENTLY PASSED AWAY

Abstract

*Composites made of resorbable polylactide modified with bone powder are part of the current search for implantable materials endowed with advantageous biomechanical functions, which make them suitable for orthopedics and traumatology applications. The bone additive containing active bone morphogenetic proteins (BMPs) and calcium phosphates introduced into the polymer matrix is to grant the implant with a biological activity. Subsequently, the resorbable matrix should get replaced with bone tissue. In order to avoid losing the osteoinductive properties of the designed material, it should be processed at low temperatures via physicochemical methods. This paper is devoted to the preparation and optimization of the composite production method suitable for biodegradable polymers and morphogenetic proteins along with the assessment of biocompatibility and biological properties of obtained materials. The tape-casting method was successfully applied. Resorbable polymer (medical poly-L-lactide, Purasorb PL38 by Purac) with 15 wt% of human bone powder (from tissue bank) were used to fabricate PLA-CP/BMPs composite implants. They were tested in *in vivo* studies that were performed in rabbit bone tissues. The results show a high biocompatibility of the material and good osteointegration with bone tissue.*

Keywords: bioactive composite, resorbable polymers, polylactide, GBR - guided bone regeneration, bone graft, BMP - bone morphogenetic proteins, osteofixation devices

doi:10.34821/eng.biomat.162.2021.13-19

[Engineering of Biomaterials 162 (2021) 13-19]



Copyright © 2021 by the authors. Some rights reserved.
Except otherwise noted, this work is licensed under
<https://creativecommons.org/licenses/by/4.0>

Introduction

Tissue grafting has been a recognized therapeutic method for many years. Bone grafts are widely used in many fields of medicine, e.g. in maxillofacial surgery, orthopedics, neurosurgery, or plastic surgery. Transplants are usually used as fillers of bone defects that result from a resection of cancerous lesions or in dental implantations. The osteoinductive properties of the grafts, i.e. the ability to stimulate the proliferation and differentiation of the recipient's bone precursors, lead to complete reconstruction and replacement of the graft tissue with the patient's own bone tissue [1]. During the process, bone morphogenetic proteins (BMPs), which are growth factors, are released from the bone matrix and stimulate osteoblasts to produce new bone tissue. Due to their osteoinductive potential, BMPs play an extremely important role in the regeneration of bone tissue [2,3]. Therefore, ground bone containing BMPs is very often used to fill cavities created after bone fragments resection. In such procedure, small bone flakes or chips are packed to fill in the space of the cavity. Unfortunately, the size of the defect treated with a ground bone is limited, and the mechanical properties of such a filling are very poor, almost none. So far, there is no processing method to form a bulk material out of a ground bone, and thus, implants in the shape of rods, cubicles, or cylinders made of this material are not available.

The possible way to exploit the natural/biological advantages of the BMPs is the fabrication of a hybrid polymeric composite. For medical applications, the most popular are bioresorbable polymers and their composites, although these materials do not have osteoinductive properties and their biocompatibility is not sufficient. The degradation rate does not match the tissue regeneration processes, and quite often the regenerating tissue differs from the primary and surrounding one (fibrous instead of cancellous). Sometimes, after the biodegradation process is finished, a hollow space (cavity) may develop, reducing the mechanical strength of the patient's bone. This cavity can be filled with tissue fluid (fluid cyst), with a noticeable inflammation around the implant, having an adverse effect on the healing process [4].

Considering that, incorporation of bone chips containing BMPs into the biopolymer matrix should improve the characteristics of the material and appears to be a key to obtain malleable materials of desired shapes and sizes. Especially given the fact that polymer composites modified with bioceramic particles are well-known and have been successfully applied over the years.

The most popular polymer used for the resorbable implants fabrication is polylactide (PLA) and its copolymers [5-8]. In order to improve the response of bone tissue to foreign body, the polymer is modified with bioactive additives, such as hydroxyapatite (HAp) or tricalcium phosphate (TCP) [9-11]. These additives have an osteoconductive effect and improve osseointegration. This phenomenon is related to the chemical similarity of the phosphates present in the implant with the minerals that build the bones. A higher degree of osteoinductive bioactivity is possible when the material is enriched with a biological agent, and bone morphogenetic proteins (BMPs) seem to be a very good choice [12,13].

Because PLA is a thermoplastic polymer, simple and efficient methods, such as extrusion or injection molding, are usually applied to obtain various shapes of implants made of this thermoplast and its composites [14,15]. These processes need high temperatures to plasticize polymers (160-240°C). Proteins like BMPs have low thermal resistance and they denature when heated over 40°C; thus, in this case, high-temperature methods cannot be used.

In the field of low-temperature polymer processing, tape casting from the solution is widely used. This method is based on solvent solution preparation (liquid) which is poured and casted in a flat die, forming a layer. When the solvent evaporates, the material dries and solidifies. As a final result, a thin foil or sheet of the material is obtained. Unfortunately, because of that, this method cannot be applied if solid (bulk) three-dimensional shapes have to be formed. Another drawback of this method is related to the substrates that are used. The preparation of the polylactide solution involves the application of toxic solvents (e.g. dichloromethane, chloroform), thus the safe usage of the prepared material in medical applications requires absolute and complete solvent evaporation during the solidification process.

This paper focuses on the fabrication of a hybrid synthetic-natural composite bulk implant, using an adapted tape casting method. As a result, the composite composed of polylactide matrix, embedded with bone chips containing BMPs, was manufactured. The authors used a pile of stacked-up, thin composite foils, bonded with a solvent, and pressed together to form cylindrical samples. Unfortunately, this approach carried a risk of solvent trapping inside an implant what can reveal unwanted side effects. The main goal of the presented work was to verify a methodology of preparation of hybrid composite bulk samples, using a modified tape casting method, and to assess the biocompatibility of the prepared composite in *in vivo* tests.

Materials and Methods

Manufacturing composite material

The hybrid-composite material was obtained by physico-chemical methods. Bioresorbable polymer (homopolymer poly-L-lactide PL38 PURASORB® by Purac, The Netherlands) and human cortical bone chips (Central Tissue Bank in Warsaw, Poland) were used. The bone was ground (average particle size ~200 μm) and defatted at ambient temperature according to standard procedures. The tape casting method was applied to obtain thin composite films (FIG. 1a). Firstly, 1 g of PLA was dissolved in 15 ml of dichloromethane. Secondly, the solution was placed on the magnetic stirrer. After 24 h, 15 wt% of ground bone was added and mixed. The solution was poured and molded into Petri dishes (dia. = 14.5 cm) creating ~0.5 mm thick layer and left for 24 h at room temperature to solidify.

Next, to achieve complete removal of possible residuals of solvent 12-hour vacuum drying was applied. When the foils were ready, round-shaped flakes were cut out (dia. 4 mm). Bulk cylinders (FIG. 1b) were formed by placing cut-out flakes in the metal tubular die. Each flake was covered on both sides with dichloromethane. Piled and stacked up flakes created a multilayer cylinder. The die was then closed with the piston and the flakes pile was compressed (1 MPa). After 24 h, the bulk sample was removed from the die and then a two-stage drying process was followed. The samples were left in the open air at room temperature for 24 h and then for an additional 24 h, they were placed in the vacuum dryer. At the end, the samples were sterilized with plasma.

In vivo test

The *in vivo* test surgical procedure was approved by the Local Ethics Committee on Animal Research by University of Life Sciences in Lublin (No 12/2014) and carried out in strict accordance with the guidelines for the care and use of experimental animals. In this study, the animals were ten healthy, skeletally mature (8-9 months of age) New Zealand White Rabbits, male, weighing 3.5-4 kg. The animals were housed in the vivarium of the University of Life Science in Lublin, under standard conditions of housing, feeding, and handling for laboratory animals. The rabbits were kept in individual cages and had free access to water and food. The surgery was performed after two weeks of quarantine. The animals were anesthetized with a mixture of xylazine (5 mg/kg *i.m.*) and ketamine (30 mg/kg *i.m.*) and subsequently by continuous infusion of the mixture of ketamine (30 mg/kg) in 5% glucose (40 mL/kg/h *i.v.*). Under aseptic conditions, a standard surgical approach to the proximal metaphyseal tibia was performed. After separating the periosteum and exposing the bone, the critical size defect (4 mm in diameter, 6 mm in depth) was drilled approximately 3 cm below the epiphyseal cartilage line. Before implantation, the defect was cleansed with a saline solution to remove any tissue debris from the cavity. The biomaterial was then inserted using the press-fit technique. Then, the skin was sutured and a postoperative radiological examination performed (Intemedical Basic 4003 device, exposure parameters were 4 mA, 50 kV). Butorphanol (0.2 mg/kg *s.c.*) for analgesia and Enrofloxacin (5 mg/kg) were administered for 3 days after the surgery to prevent probability of infection.

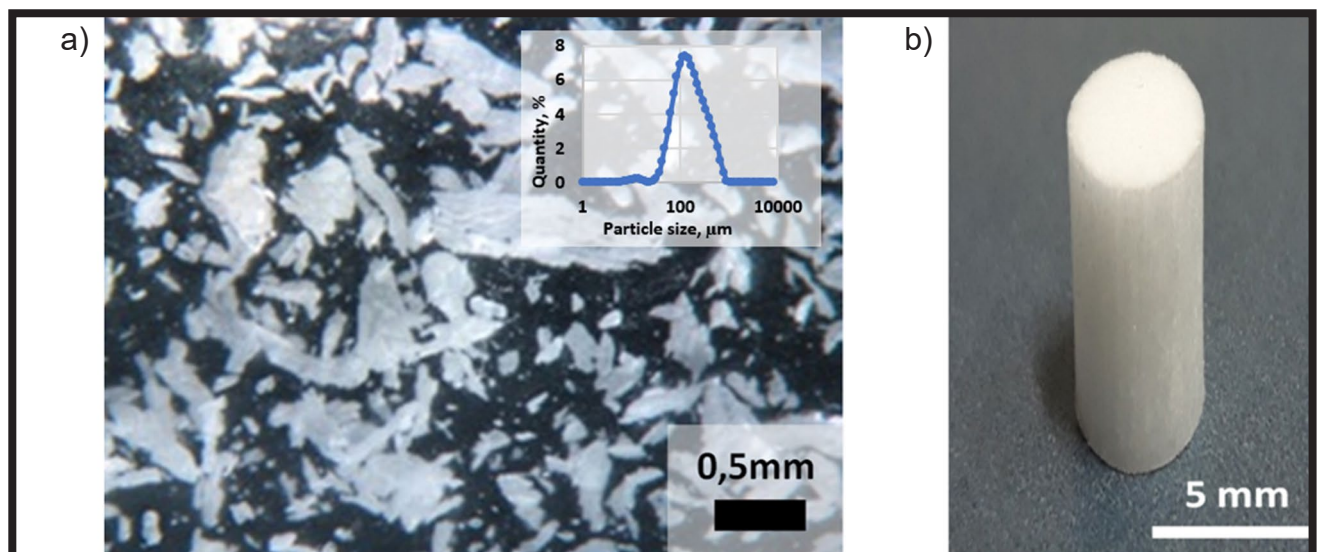


FIG. 1. Images of: a) PLA-bone composite foil with 15 wt% of bone additive (optical microscopy) with particle size analysis, b) implanted cylinder of PLA-bone.

The rabbits were sacrificed 12 weeks after surgery with an overdose of sodium pentobarbital (Morbital 1 ml/kg *i.v.*). Then a radiological examination was performed and specimens were collected for histological and SEM evaluation.

Microscopic observation

The biological preparations (FIG. 2a) were prepared using a low-speed diamond saw, then dried at room temperature and sputtered with carbon. The material was evaluated by means of SEM microscopy using a NOVA NANO SEM 200 microscope. An EDS analysis of the cross sections of the samples was also carried out.

Histopathological examination

Bone tissue was partially decalcified in the electrolytic decalcifying solution produced by Bio-Optica. Then it was placed in paraffin blocks (FIG. 2b) according to standard procedures [16] and cut into 4 μ m sections using a microtome. Having been cut, the sections of the bone tissue were routinely stained with HE (hematoxylin and eosin). The preparations were scanned with the Hamamatsu NanoZoomer 2.0-HT scanner and evaluated using the NDP.view2 software.

Results and Discussion

Results

Evaluation of implantation healing process

There were no intraoperative complications either at the time of implantation or during the entire treatment period. Furthermore, no signs of inflammation or adverse tissue reactions around the implantation site were observed during the tests.

Macroscopic observation revealed completely filled bone defects with no empty spaces between implanted material and bone tissue. The small amount of biomaterial was still visible on the surface of the new bone tissue. There were no pathological macroscopic changes either in the soft tissue surrounding the implantation site or in the popliteal lymph nodes.

Radiographic examination

After 12 weeks from the operation, the bone defects were completely filled by the newly formed bone tissue and the small amount of residual biomaterial. The cortical layer of the bone defect was reconstructed. No radiological signs of any adverse reaction to the implant were observed (FIG. 3).

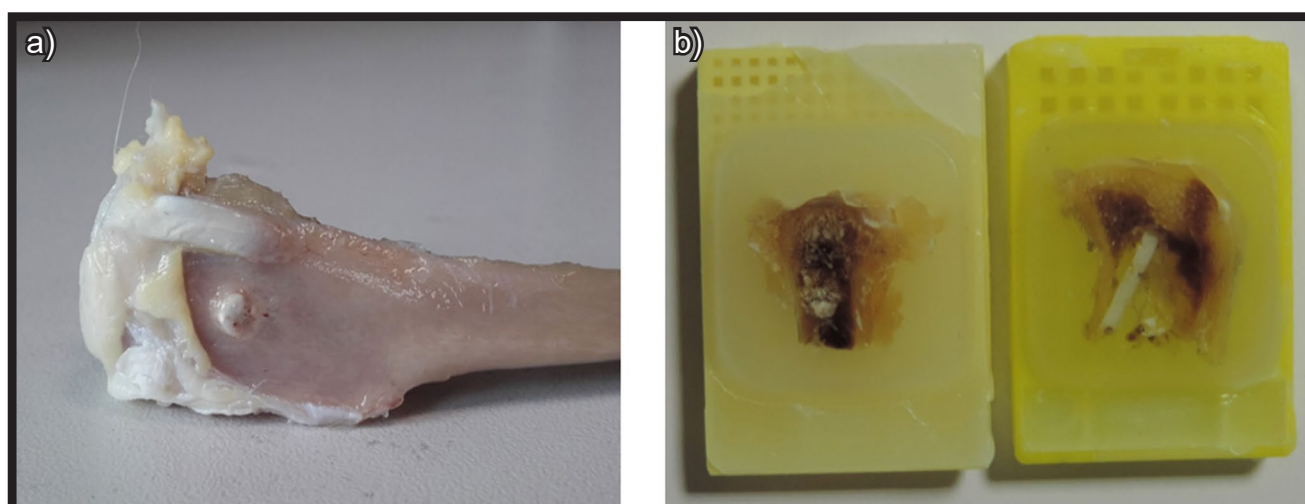


FIG. 2. a) The composite implant in the bone tissue – 12 weeks after surgery; b) Paraffin blocks containing bone tissue.

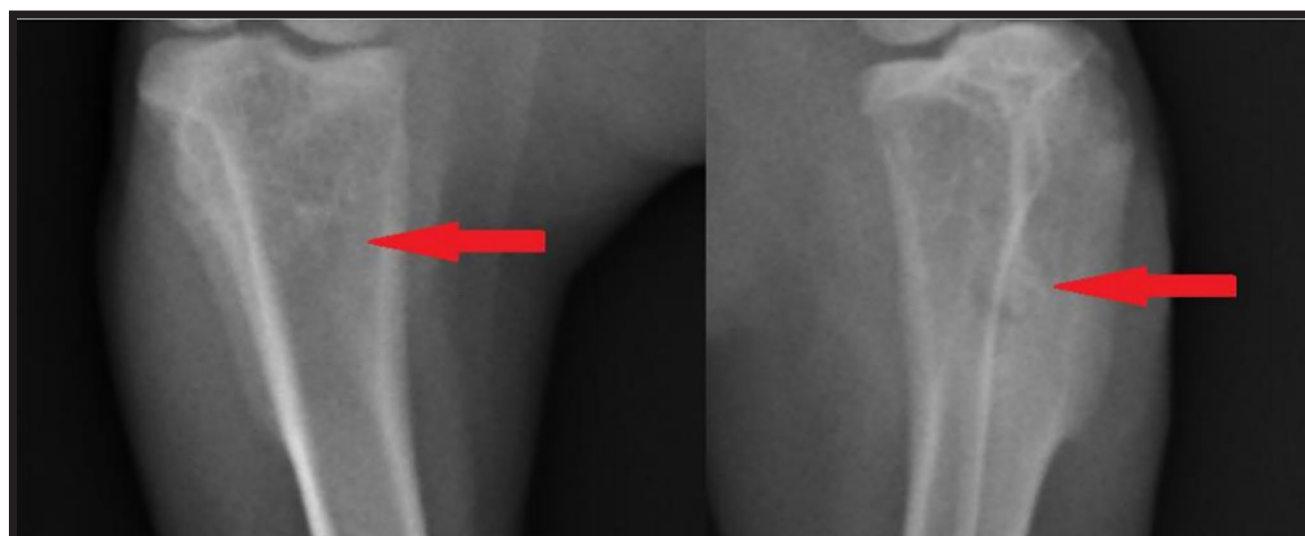
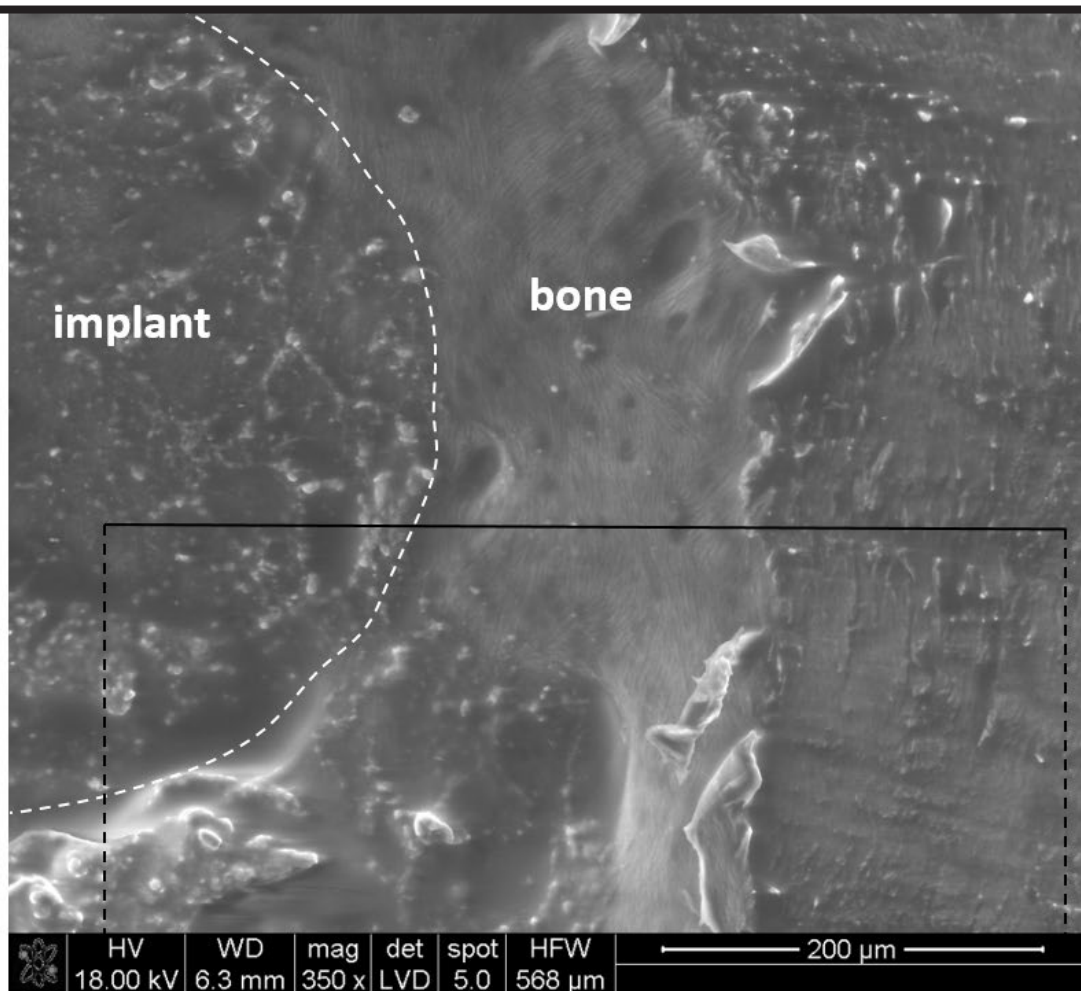


FIG. 3. Radiological images of bones with implants 12 weeks after implantation (implants are hardly visible due to their X-ray transparency and are marked with arrows).

a)



b)

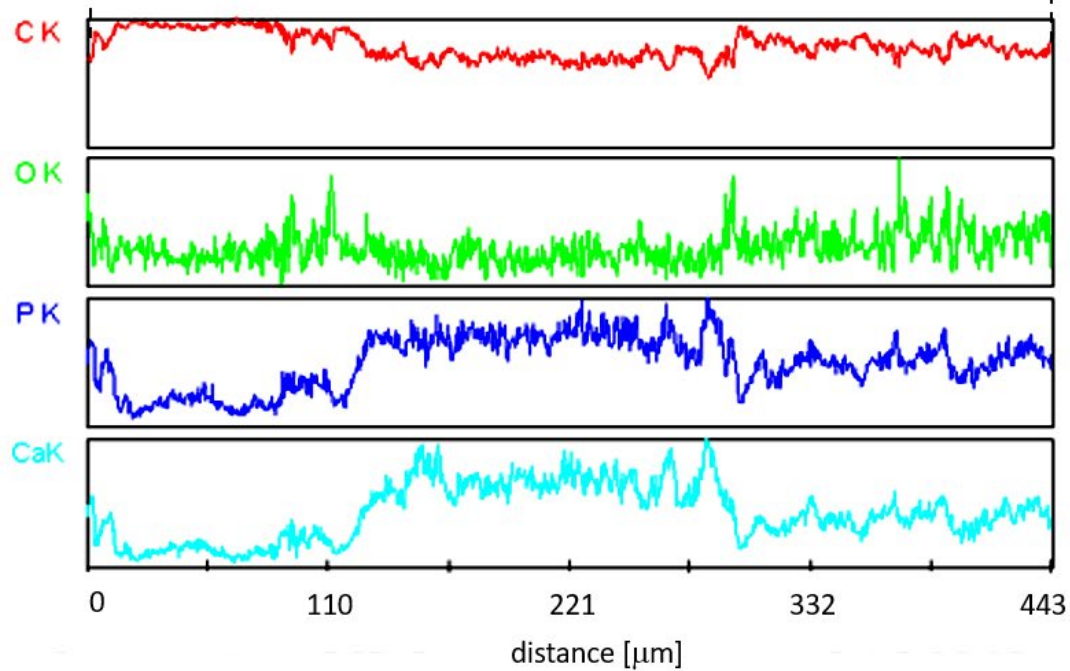


FIG. 4. a) SEM image of bone-implant section; b) EDS analysis of element composition (carbon, oxygen, phosphorus, calcium) along the line marked on the SEM image.

Microscopic observations of bone fractures (cross sections) performed 12 weeks after implantation confirmed the efficient connection of the implant with the bone (FIG. 4a). The absence of a fibrous envelope indicates the biocompatibility of the implant. The EDS analysis of the element composition along the line running from the implant to the bone (FIG. 4b) reveals the presence of calcium and phosphorus - mainly in the bone tissue, but also within the implant. At the same time, there is no noticeable change in the composition at the bone-implant connection site.

Histopathological evaluation was based on the tissue reaction around the examined material. In FIG. 5 the implanted material is visible (the spot marked with two circles), and FIGS 6 and 7 present the tissues directly adjacent to the implant. Several types of tissue changes were observed, none of them of undesirable character. In the vicinity of the implant, fibrous tissue was observed (FIG. 5) along with the new bone structure and increased osteogenic activity of neighboring bone trabeculas. A focal nonspecific granulomatous reaction of the "foreign body" type with visible multinucleated giant cells (FIG. 6) was not revealed in the immediate vicinity of the implant. None of the fields analyzed showed either an acute inflammatory response (without granulocytes) or a chronic inflammatory response (without lymphocytic infiltration). The samples did not reveal signs of necrosis, haemorrhage or other forms of tissue damage.

Discussion

The medical application of BMPs has been the subject of scientific works since the 1970s, raising both high hopes and various fears. Many authors indicate that morphogenetic proteins play an important role in bone tissue repair processes. An increase in the concentration of these proteins is observed in patients suffering from bone fractures [17]. *In vivo* studies prove the beneficial effect of proteins on the reconstruction of collagen, especially in cases of earlier estrogen deficiency and coexisting osteoporosis [18]. This is particularly important when treating patients with the pathologically changed bone tissue. At the same time, the presence of bio-based components in implants may raise recipients' concerns. Some patients may object to the application of human bone from the tissue bank, either for ethical reasons, the risk of disease transmission, or an unwanted biological response.

Bearing in mind all these considerations, in order to improve the biological response of bone tissue, especially in patients with reduced regenerative abilities, it seems reasonable to investigate the use of BMPs of natural origin (from native bone) as modifying factors of polymeric matrix, for example PLA.

An additional challenge is the fabrication of implants made of such composites, which would possess efficient biomechanical properties and could be formed into complex three-dimensional shapes (e.g. screws, nails, plates, or pins). On the one hand, there are forming methods such as extrusion or injection molding which would be appropriate for this task, but on the other hand, the temperatures applied in these processes (160-240°C) exclude incorporation of BMPs because of their low thermal resistance (up to 40°C).

As shown in this article, it is possible to prepare a hybrid composite material of PLA matrix, modified with embedded bone chips containing BMPs, which maintain their bioactivity. The authors adopted a tape casting method to form thin foils of composite material, and by piling them layer-on-layer, and pressing together, bulk cylindrical samples were made. It is presumed that bulk composite (green body) can be formed into screws or fixation plates by the machining process, but so far nothing can be said about the mechanical behavior and properties of such implants.

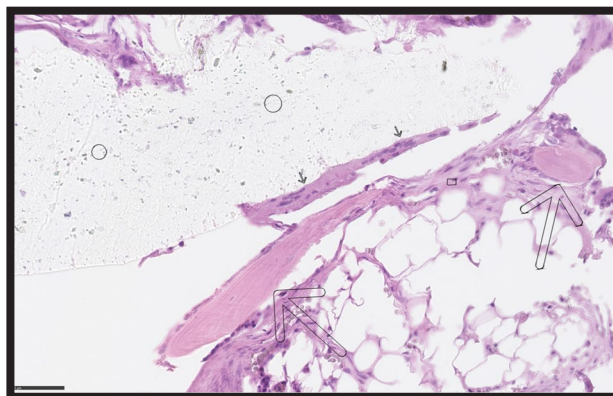


FIG. 5. Foci of bone formation, fibrosis and granulomatous reaction in the vicinity of the examined material (BM) - the implant marked with the circles (transparent area), the giant polynuclear cells with small arrows, the bone formation areas with large arrows.

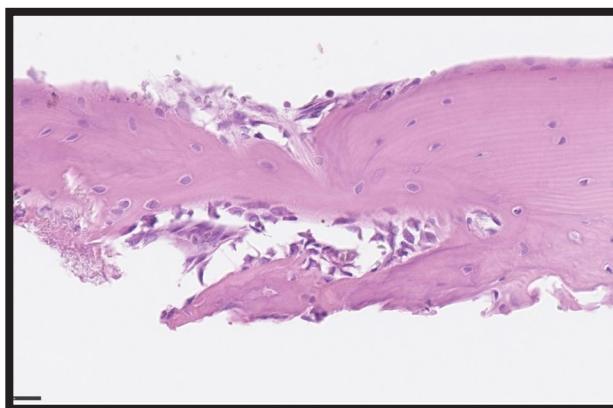


FIG. 6. Increased osteogenic activity in the bone trabeculas (on the edge of the osteoblast and newly-formed bone).

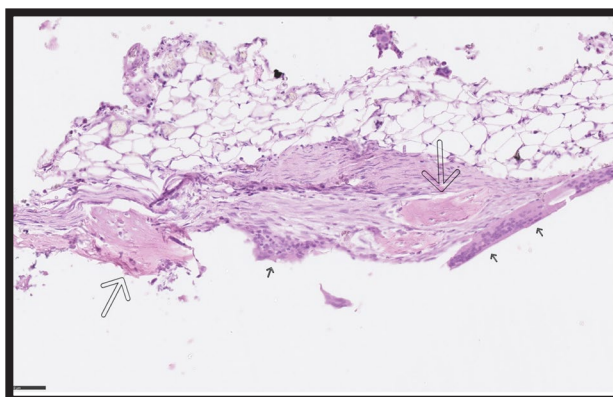


FIG. 7. Tissue in the immediate vicinity of the implant with foci of bone formation (large arrows), fibrosis and granulomatous reaction with the presence of cells around the foreign body (small arrows).

TABLE 1. Selected features of various materials [4,20-23].

Material	Osteoinduction	Bioactivity	Malleability	Formability
Cortical bone	✓	<i>Biological</i> <i>Chemical</i>	x	x
Cancellous bone				
BMP	✓	<i>Biological</i> <i>Chemical</i>	x	x
HAp	✓	<i>Chemical</i>	x	x
TCP				
PLA	x	x	✓	✓
PLA – CP (HAp, TCP)	✓	<i>Chemical</i>	✓	✓
PLA – CP/BMPs	✓	<i>Biological</i> <i>Chemical</i>	✓	x

The biological aspects of the obtained composite are considered by comparison with bone and other materials widely used for medical applications. TABLE 1 presents the characteristics of bone, BMPs, HAP and TCP, polylactide and composites with a polylactide matrix modified with HAP (PLA-CP/HAP), a polylactide matrix modified with TCP (PLA-CP/TCP), and a polylactide matrix modified with bone chips with osteoinductive supplements and BMPs (PLA-CP/BMPs).

When implanted, calcium phosphates (CP) like HAP and TCP (powder, granules, porous or bulk), reveal osteoconductivity. Because of their chemical similarity to bone tissue, they are very good bone-substitute materials. However, they are ceramics, and thus, their formability and malleability are limited. When HAP or/and TCP are introduced into the polymer matrix (PLA-CP/HAP, PLA-CP/TCP), the as-obtained composite can be easily formed and shaped by extruding or injection moulding. Such implants have rather sufficient mechanical properties, but their application is limited to non-load-bearing implantation sites [19]. They pose osteoconductivity with a controlled degradation rate of the polymer matrix. Judging by the comparison presented in TABLE 1, the best material among the listed seems to be the composite PLA-CP/BMPs. It is supposed to be chemically and, more importantly, biologically active. Having morphogenetic proteins inserted in the polymeric matrix, this composite induces regeneration of natural tissue on various levels. That is why it is better than the other materials compiled in TABLE 1.

The biological behavior of the prepared composite samples was tested in *in vivo* test. No empty spaces between the implanted material and the bone tissue were observed, and no pathological macroscopic changes, either in the soft tissue surrounding the implantation site, or in the popliteal lymph nodes were discovered. The biocompatibility of the implant was confirmed by the absence of a fibrous envelope and a complete filling of the bone defect by the newly formed bone tissue. The EDS analysis showed the presence of calcium and phosphorus within the implant what indicates the bone cell infiltration into the material structure. Because no unwanted reactions or side effects occurred, the authors claim that the multi-stage long-time drying applied after the tape casting preparation is an efficient method for removing all residuals of toxic solvent from the implant.

Conclusions

1. Bulk composite materials made of the resorbable polymer (medical poly-L-lactide, Purasorb PL38 by Purac), modified with 15 wt% human bone chips containing BMPs (from the tissue bank) were successfully obtained by tape casting, vacuum drying, foils piling, and pressing.

2. Composite PLA-CP/BMPs is modified with native ground bone, thus natural calcium phosphates and morphogenetic proteins are present. Combination of these factors gives the composite a high biological activity.








3. *In vivo* studies proved that the implants enriched with active morphogenetic factor (BMPs) derived from natural bone tissue possess high biocompatibility and stimulate good osteointegration.

4. Further research should focus on the fabrication of complex-shaped implants (nails, screws, plates) by machining of bulk pieces of PLA-BMPs composite, and their mechanical characterization. Such implants may be a promising alternative to traditional metal implants.

Acknowledgements

This work was supported from the subsidy of the Ministry of Education and Science for the AGH University of Science and Technology in Kraków (Project No 16.16.160.557).



ORCID iDs

B. Szaraniec:	 https://orcid.org/0000-0002-9231-4976
T. Szponder:	 https://orcid.org/0000-0001-7949-7328
K. Gryń:	 https://orcid.org/0000-0001-6499-2465
M. Ambroziak:	 https://orcid.org/0000-0002-3570-672X
G. Gut :	 https://orcid.org/0000-0002-7164-4298
Ł. Koperski	 https://orcid.org/0000-0001-8163-1813
J. Chłopek	 https://orcid.org/0000-0003-3293-9082

References

- [1] Huntley R., Jensen E., Gopalakrishnan R., Mansky K.C.: Bone morphogenetic proteins: Their role in regulating osteoclast differentiation. *Bone Rep.* 10 (2019) 100207.
- [2] Guo L., Min S., Su Y. et al.: Collagen sponge functionalized with chimeric anti-BMP-2 monoclonal antibody mediates repair of nonunion tibia defects in a nonhuman primate model: An exploratory study. *Journal of Biomaterials Applications* 32 (2017) 425-432.
- [3] Matsumoto G., Ueda T., Sugita Y.T.: Polyhedral microcrystals encapsulating bone morphogenetic protein 2 improve healing in the alveolar ridge. *Journal of Biomaterials Applications* 30 (2015) 193-200.
- [4] Chłopek J., Kmita G.: Non-Metallic Composite Materials for Bone Surgery. *Engineering Transactions* 51 (2003) 307-323.
- [5] Nair L.S., Cato T.L.: Biodegradable polymers as biomaterials. *Progress in Polymer Science* 32 (2007) 762-798.
- [6] Pillai C.K., Sharma C.P.: Absorbable Polymeric Surgical Sutures: Chemistry, Production, Properties, Biodegradability and Performance. *Journal of Biomaterials Applications* 25 (2010) 291-366.
- [7] Parra M., Moya M.P., Rebolledo C., Haidar Z.S., Alister J.P., Olate S.: PLA/PGA and its co-polymers in alveolar bone regeneration. A systematic review. *Int. J. Odontostomatol.* 13(3) (2019) 258-265.
- [8] Dedukh N.V., Makarov V.B., Pavlov A.D.: Polylactide-based biomaterial and its use as bone implants (analytical literature review). *Pain, Joints, Spine* 9 (2019) 28-35.
- [9] Szaraniec B.: Durability of Biodegradable Internal Fixation Plates. *Materials Science Forum* 730-732 (2013) 15-19.
- [10] Gryń K., Szaraniec B., Morawska-Chochol A., Chłopek J.: Mechanical characterization of multifunctional resorbable composite plate for osteosynthesis. *Engineering of Biomaterials* 18 (2015) 22-33.
- [11] Backes E.H., de Nóbile Pires L., Selistre-de-Araujo H.S., Costa L.C., Passador F.R., Pessan L.A.: Development and characterization of printable PLA/β-TCP bioactive composites for bone tissue applications. *J Appl Polym Sci.* 138 (2020) 49759.
- [12] Lademann F., Hofbauer L.C., Rauner M.: The Bone Morphogenetic Protein Pathway: The Osteoclastic Perspective. *Front. Cell Dev. Biol.* 8 (2020) 586031.
- [13] Nauth A., Ristiniemi J., McKee M.D., Schemitsch E.H.: Bone morphogenetic proteins in open fractures: past, present, and future. *Injury* 40 (2009) 27-31.
- [14] Fialho S.L., da Silva Cunha A.: Manufacturing Techniques of Biodegradable Implants Intended for Intraocular Application. *Drug Delivery* 12 (2005) 109-116.
- [15] de Melo L.P., Salmoria G.V., Fancello E.A., de Mello Roesler C.R.: Influence of Processing Conditions on the Mechanical Behavior and Morphology of Injection Molded Poly(lactic-co-glycolic acid). *International Journal of Biomaterials* 85 (2017) 6435076.
- [16] Kang Q.K., LaBreck J.C., Gruber H.E., An Y.H.: Histological Techniques for Decalcified Bone and Cartilage. In: An Y.H., Martin K.L. (eds) *Handbook of Histology Methods for Bone and Cartilage.* (2003) Humana Press, Totowa, NJ.
- [17] Dai J., Li L., Jiang C., Wang C., Chen H., Chai Y.: Bone Morphogenetic Protein for the Healing of Tibial Fracture: A Meta-Analysis of Randomized Controlled Trials. *PLoS ONE* (2015) 10.
- [18] Kanakaris N.K., Petsatodis G., Tagil M., Giannoudis P.V.: Is there a role for bone morphogenetic proteins in osteoporotic fractures? *Injury* 40 (2009) 21-26.
- [19] Gryń K.: Long-term mechanical testing of multifunctional composite fixation miniplates. *Engineering of Biomaterials* 157 (2020) 20-25.
- [20] Jeong J., Kim J.H., Shim J.H., Hwang N.S., Heo C.Y.: Bioactive calcium phosphate materials and applications in bone regeneration. *Biomater Res.* 23 (2019) 1-11.
- [21] Katagiri T., Watabe T.: Bone Morphogenetic Proteins. *Cold Spring Harb Perspect Biol.* 8 Published (2016) 021899.
- [22] Buser Z., Brodke D.S., Youssef J.A., et al.: Allograft Versus Demineralized Bone Matrix in Instrumented and Noninstrumented Lumbar Fusion: A Systematic Review. *Global Spine Journal* 8 (2018) 396-412.
- [23] Fernandez de Grado G., Keller L., Idoux-Gillet Y., et al.: Bone substitutes: a review of their characteristics, clinical use, and perspectives for large bone defects management. *J Tissue Eng.* 9 (2018) 1-18.

EMULSION ELECTROSPINNING – METHOD TO INTRODUCE PROTEINS FOR BIOMEDICAL APPLICATIONS

ROKSANA KURPANIK^{1*} , ALICJA RAPACZ-KMITA² ,
ANNA ŚCISŁOWSKA-CZARNECKA³ ,
EWA STODOLAK-ZYCH¹ 

¹ DEPARTMENT OF BIOMATERIALS AND COMPOSITES,
FACULTY OF MATERIALS SCIENCE AND CERAMICS,
AGH UNIVERSITY OF SCIENCE AND TECHNOLOGY,
AL. MICKIEWICZA 30, 30-059 KRAKOW, POLAND

² DEPARTMENT OF CERAMICS AND REFRACTORIES,
FACULTY OF MATERIALS SCIENCE AND CERAMICS,
AGH UNIVERSITY OF SCIENCE AND TECHNOLOGY,
AL. MICKIEWICZA 30, 30-059 KRAKOW, POLAND

³ DEPARTMENT OF COSMETOLOGY, INSTITUTE OF APPLIED
SCIENCES, FACULTY OF MOTOR REHABILITATION,
UNIVERSITY OF PHYSICAL EDUCATION IN KRAKOW,
AL. JANA PAWŁA II 78, 31-571 KRAKOW, POLAND

*E-MAIL: KURPANIK@AGH.EDU.PL

Abstract

The aim of this work was to obtain polymer fibers by the emulsion electrospinning. For this purpose, polycaprolactone (PCL) was used, which was modified before the electrospinning stage with micelles obtained by the oil-in-water (O/W) emulsion method. Micelles were obtained by combining the non-ionic surfactant Tween 80 or Triton X-100 used at different concentrations with the amino acid alanine. The obtained fibrous substrates had a typical unimodal fiber size distribution and their average size was in the range of 590-800 nm. The effectiveness of the emulsion electrospinning process was confirmed by Fourier Transform Infrared Spectroscopy - Attenuated Total Reflectance (FTIR-ATR) showing the presence of surfactants. The addition of micelles to the polymer solution significantly reduces the contact angle of nonwoven fabrics: from 120° (for PCL) to ~20-30° for surfactant-loaded nonwovens, and the micellar form allows tracking the release of alanine into the solution (UV-Vis). The combination of the core-shell-morphology of the emulsion electrospun fibers allows comparable amino acid release times. There were no significant differences in both the amount of alanine released and the rate of its release between PCL/Tween80/alanine and PCL/Triton X-100/alanine fibers, which were characterized by a similar fiber size.

Keywords: emulsion electrospinning, alanine, polycaprolactone, Tween 80, Triton X-100, micelle

doi:10.34821/eng.biomat.162.2021.20-25

[Engineering of Biomaterials 162 (2021) 20-25]



Copyright © 2021 by the authors. Some rights reserved.
Except otherwise noted, this work is licensed under
<https://creativecommons.org/licenses/by/4.0>

Introduction

The possibility to produce nanofiber scaffolds that mimic the microstructure of the extracellular matrix (ECM) is an advantage of electrospinning techniques used in tissue engineering and regenerative medicine. Modification of electrospinning parameters: environmental, apparatus as well as the possibility of modifying the solution used to produce nanofibers gives new opportunities to prepare scaffolds with the desired behavior in a living organism. This is especially important when tissue regeneration requires a special approach i.e. targeted drug delivery or release of bioactive agents. Promoting cell adhesion, proliferation, migration and ingrowth are one of the main requirements of tissue engineering. There are many methods to stimulate an appropriate response of cells to the scaffold, including growth factors, adhesive peptides, ECM proteins, cytokines, hormones, or genes [1,2].

The main role of incorporating these molecules is to provide binding sites for cells, and such an approach allows to mimic not only the microstructure of the extracellular matrix but also its chemistry and signaling, thus ensuring a better similarity to the natural tissue microenvironment [1,3]. Peptide-based scaffolds are gaining more and more interest as an alternative to proteins due to their structural and biological similarity. In addition, these biomolecules are easier to introduce and more resistant to environmental conditions than larger proteins. Amino acids are modifiers that also have a beneficial effect on cells, and as the basic building blocks of proteins, they influence processes such as cell growth, differentiation, and metabolism. Research shows that amino acids, including methionine, leucine, and glutamine, act as activators of growth pathways [4]. Another amino acid that plays an important role in cell growth and T-cells activation is alanine, and its deprivation leads to impairment of cell growth, proliferation, and function [5]. These advantages make it an attractive biomodifier to stimulate an appropriate cellular response to the implant surface. There are many methods to incorporate bioactive molecules into fibers, which include their external immobilization and encapsulation within them. Due to their controlled release kinetics, core-shell nanofibers are gaining tremendous interest as a substrate for cell proliferation. Moreover, the encapsulation of proteins and pharmaceuticals in electrospun fibers is one of the strategies to overcome the barriers associated with maintaining the stability and effectiveness of the active ingredient during the formulation process [6]. The methods of producing core-shell fibers mainly include blend electrospinning or coaxial electrospinning. The first technique, which consists in dissolving both components in a suitable solvent, has the fastest loading rate compared to the other methods. However, due to the use of an organic solvent, there is a risk of denaturing bioactive molecules. Furthermore, diffusion of the encapsulated particles to the peripheral parts of the fibers contributes to the burst release effect [7,8]. Contrary to this technique, coaxial electrospinning, due to separate solution delivery systems, allows for the use of a wider range of polymers for the core part and the shell, as well as for the diversified distribution of biomolecules in the fibers and their release kinetics [9]. However, there is still the possibility of diffusion of the bioagent into the shell part during the formation of the Taylor cone, which leads to a non-linear release kinetics [8]. Emulsion electrospinning is another modification that is used to produce nanofibers that release biologically active compounds or drugs. This simple method is based on the use of an oil-in-water (O/W) or water-in-oil emulsion (W/O) as the electrospinning solution, and a surfactant (which acts as an emulsifier) is used to stabilize the emulsion.

Moreover, the type (ionic, non-ionic) and concentration of the surfactant affect the surface tension and conductivity of the solution, which ultimately affects the morphology and internal architecture of the fibers [10]. The advantage of emulsion electrospinning is control of the kinetics of the release of the active ingredient or biomolecule and high-efficiency encapsulation. Due to the use of surfactant, the bioagents are separated from the organic solvent, which reduces the risk of its denaturation and enables the combination of hydrophobic polymers with hydrophilic biomolecules [7, 11]. The advantage of emulsion electrospinning over traditional coaxial electrospinning is that it does not require additional equipment (special spinneret, separate delivery systems) for the production of core-shell fibers. Emulsion electrospinning uses a standard single-nozzle system, which makes it a more convenient and cost-effective method [12]. Due to the above-mentioned advantages, this method is often used for the encapsulation of biomolecules into synthetic polymers to increase their biocompatibility.

Polycaprolactone (PCL) due to its relatively good biocompatibility, low toxicity, and good mechanical properties, is one of the most widely used synthetic polymer in the biomedical field. However, its high hydrophobicity and low bioregulatory activity impair appropriate cellular adhesion and proliferation. Therefore, emulsion electrospinning is used to incorporate various biomolecules, such as peptides or growth factors, to increase PCL hydrophilicity and biological activity without the risk of damaging them [13]. Baskapan et al. used this method to encapsulate laminin in PCL fibers for kidney regeneration. As a result they obtained a nonwoven fabric with higher elastic properties and hydrophilicity, which resulted in better renal cell adhesion [14]. In turn, Basar et al. obtained binary system PCL/gelatin loaded with Ketoprofen mats with more sustained release kinetics in comparison to single PCL mat. The use of emulsion electrospinning enabled more sustained drug release up to 4 days and significantly inhibited burst release [13]. However, the possibility of encapsulating low molecular weight biomolecules still needs to be explored.

In our research, we focused on the possibility of loading alanine into nanofibers using emulsion electrospinning, which creates core-shell nanofibers from an emulsion consisting of an organic phase (polymer) with a surfactant and an aqueous phase (surfactant with alanine). To prevent the negative interaction of the model biomolecule (alanine) suspended in the aqueous phase with the polymer organic solvent during the electrospinning process, commercial surfactants were used (Tween 80, Triton X-100). The next step was to optimize electrospinning conditions to obtain fibers enriched with encapsulated amino acids. Specifically, we investigated the solution and emulsion process parameters for electrospinning to achieve high nanofiber biomolecule loading, prolonged formulation stability, and controlled protein release for future biomedical applications.

Materials and Methods

Preparation of the emulsion

A water-in-oil (W/O) emulsion was prepared for an electrospinning solution, with the oil and water phases being prepared separately. Polycaprolactone 10% (w/v) (PCL, Mw = 80 kDa, Sigma-Aldrich, Germany) and surfactants (Tween 80 and Triton X-100, Sigma-Aldrich) at various concentrations (0.5% v/v, 1% v/v and 5% v/v for Tween 80 and 0.5% v/v, 1% v/v and 3% v/v for Triton X-100) were dissolved in dichloromethane (DCM, Chemland SA) and dimethylformamide (DMF, Chemland SA) (volume ratio of 7:3 v/v), while alanine (L-alanine, Sigma-Aldrich, Germany) was dissolved in distilled water to prepare the water phase.

The alanine solution (5% by weight of dry PCL) was then added dropwise to the polymer solution and stirred in an ice bath. The emulsions were used for electrospinning immediately after preparation. The selection of a safe amount of surfactant was based on data from the literature. The applied amount of surfactant should not adversely affect the cellular response [15].

Preparation of the fibrous membrane by electrospinning

The electrospinning process was carried out at an ambient temperature (~25°C) and relative humidity in the range of 40–50%, and the emulsion was fed at a rate of 0.7 ml/h. The fibers were collected on 10 cm aluminium foil from the spinneret to the collector and a voltage of 18 kV was applied.

Electrospun mats characterization Physicochemical properties

The microstructure of the nanofibers was observed with a scanning electron microscope (NOVA NANO SEM 200) and the samples were coated with a 10 nm gold layer prior to observation. The diameter of 100 random fibers in each sample was measured with ImageJ software, and the fibers size distribution was obtained.

The effectiveness of the modification of polymer fibers by micelles and the presence of surfactants were investigated by Fourier Transform Infrared Spectroscopy in the ATR mode (Bruker Tensor 27 FTIR). Infrared spectra were acquired using 64 scans in the range of 4000–400 cm⁻¹ and spectra resolution of 4 cm⁻¹.

To determine the wettability of the scaffold, the contact angle was measured by a sessile drop test using a Kruss DSA 25 goniometer. Measurements were made by placing a drop (1 µL) of deionized water on the sample surface. The contact angle value was determined as the average of 10 measurements for each sample. The test was carried out at room temperature.

All prepared samples with the same weight of ~15 mg (to normalize the thickness differences) were incubated in NaCl solution for one month, and the concentration of alanine in the solution was assessed weekly by spectrophotometry (UV-Vis, Cecil 2520). A reaction with ninhydrin was performed to determine the amount of alanine released. Briefly, ninhydrin was dissolved in ethanol to obtain a 1% (w/v) solution. Then, 1 mL of incubation solution was added to 1 mL of ninhydrin solution and heated for 1 min (until colour turned violet) and placed in the spectrophotometer chamber. The determination of alanine concentration was performed at a wavelength of 570 nm and was determined from a standard curve derived from solutions of known concentration. To obtain the standard curve, the solutions with an increasing concentration of alanine were prepared (0.2 mg/mL, 0.4 mg/mL, 0.6 mg/mL, 0.8 mg/mL, 1 mg/mL) and reaction with ninhydrin was performed. Then, based on the obtained data, a regression curve was determined, which was used to determine the concentration of released alanine. Loading efficiency (LE) was calculated using the equation:

$$\%LE = \frac{\text{mass of alanine in fibers}}{\text{mass of fibers}} \cdot 100\% \quad (1)$$

Statistical analysis

All results are presented as mean ± standard deviation. To determine the significance level for the biological study, statistical analysis was conducted with one-way ANOVA followed by Tukey's post hoc analysis. Probability values less than 0.05 were considered statistically significant. The ANOVA analysis was performed using Origin Pro 2021 software.

Results and Discussion

To assess the impact of the amount of the surfactant on the fibers diameter and morphology, different concentrations of the surfactants were used. It was found that the morphology of the fibers obtained from emulsion electrospinning strongly depended on the amount of surfactant in the solution (FIG. 1). For higher concentration, defects and pores on the fibers surface were observed (FIG. 1A and 1D), while thin, smooth and uniform fibers were obtained at 1% v/v and below (FIG. 1B-C and 1E-F). The histograms presenting the fiber diameter distribution (FIG. 2A-C) indicate that the use of emulsion as a spinning solution affects the diameter of the PCL fibers. The PCL fibers diameter was in the range of 450-1100 nm for pure PCL (FIG. 2A) and the distribution was unimodal with a maximum at 400-800 nm for PCL/Tween80/alanine (FIG. 2B) and PCL/Triton X-100/alanine (FIG. 2C).

However, emulsion electrospinning contributed to the formation of fibers that mostly had diameters smaller than PCL (below 480 nm). In addition to nanometer-range fibers, fibers significantly larger than PCL (over micrometers) were also observed. The difference was also confirmed by the ANOVA test, which showed significant differences between the entire population means. However, there were no significant differences between the fibers obtained from emulsion with Tween 80 independently on the concentration (ANOVA, $p = 0.615$) which indicates the fact that the use of Tween 80 results in obtaining more uniform fibers. Moreover, depending on the size of the micelles (for PCL/Tween80/alanine $\phi_{\text{mean}} = 22 \mu\text{m}$ with polydispersity index $PI = 0.45$ and for PCL/Triton X-100/alanine was $\phi_{\text{mean}} = 31 \mu\text{m}$ and $PI = 0.97$), the fiber microstructure was different, and the fibers were either completely internally hollow or exhibited an intrinsic hierarchical porosity (FIG. 1G-H).

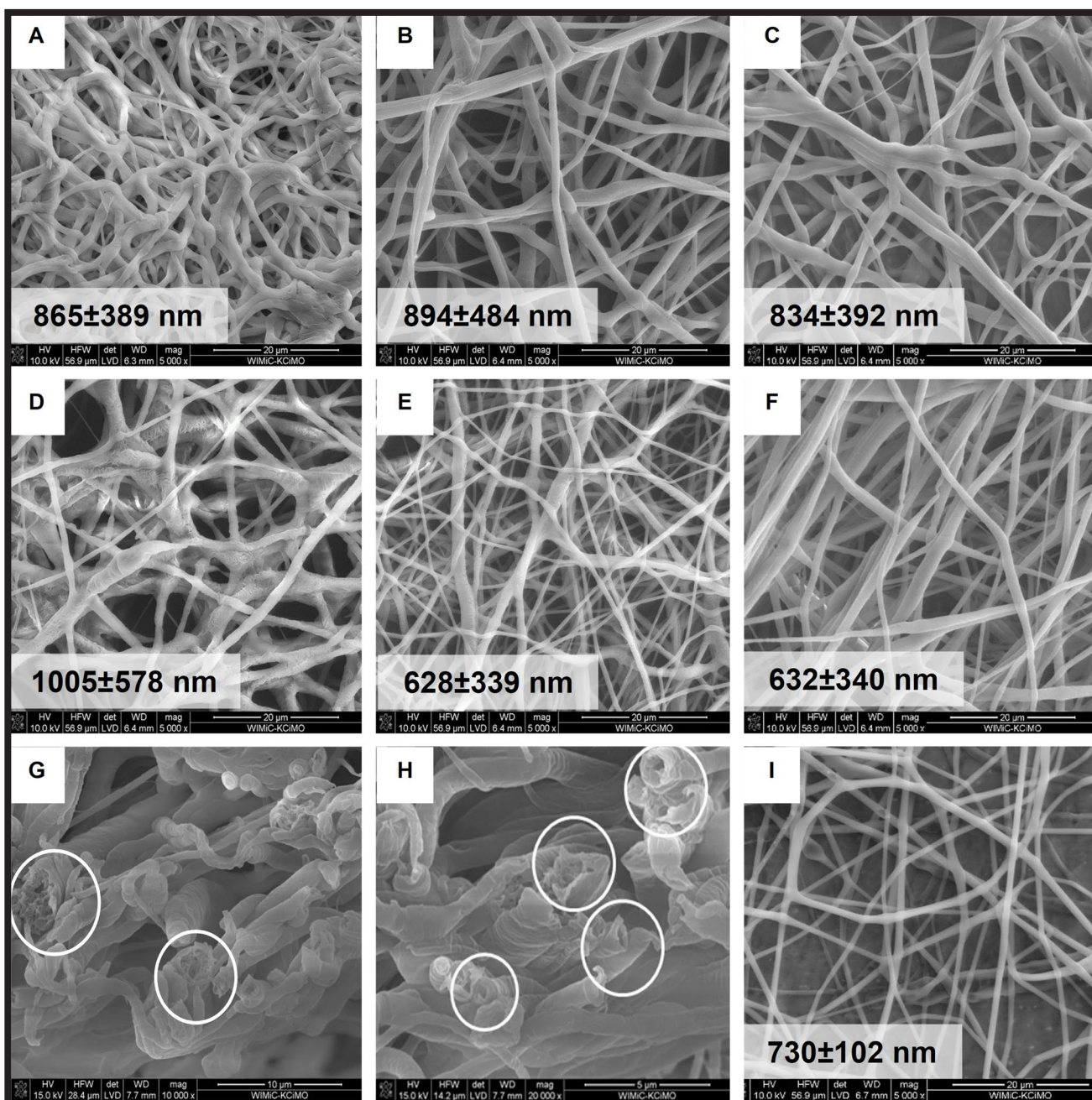


FIG. 1. SEM images and mean fiber diameter \pm standard deviation of PCL/alanine nanofibers prepared using Tween 80 at concentrations: (A) 5% v/v, (B) 1% v/v, (C) 0.5% v/v and Triton X-100 at concentrations: (D) 3% v/v, (E) 1% v/v, (F) 0.5% v/v. Cross-sections of the PCL/alanine nanofibers prepared using: (G) 1% v/v Tween 80, (H) 1% v/v Triton X-100. Image (I) presents neat PCL fibers.

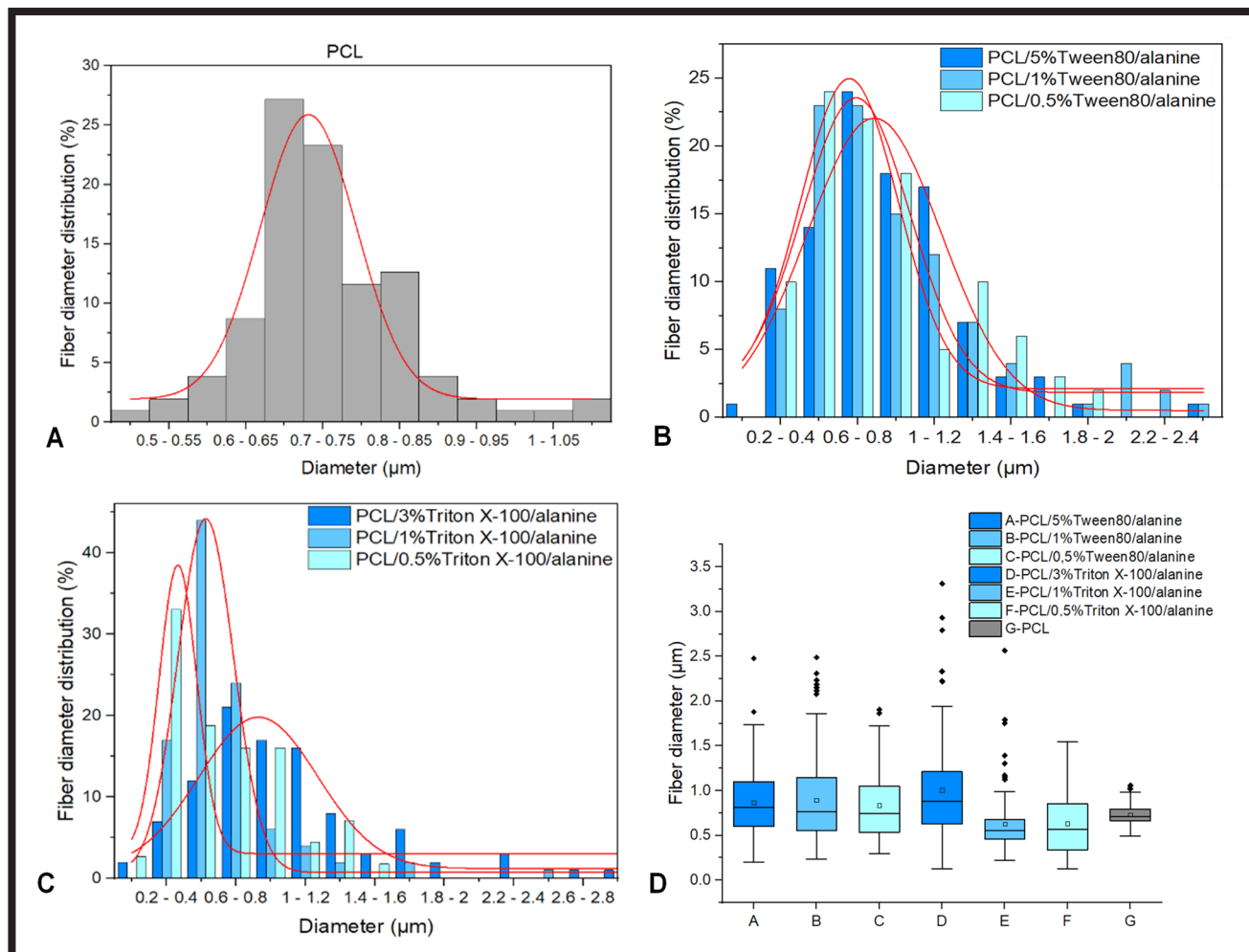


FIG. 2. Diameter distribution of (A) neat PCL, (B) PCL/Tween80/alanine, (C) PCL/Triton X-100/alanine fibers and (D) mean diameters of the fibers. Based on $n = 100$ measurements.

A similar internal microstructure was obtained by Johnson et al. only by addition of the surfactant [16]. This may indicate that some of the surfactants not bound to alanine created closed pores inside the fibers.

The FTIR-ATR spectra of emulsion electrospun membranes are presented in FIG. 3. Since the same FTIR spectra for all samples were acquired and the high concentration of surfactant results in the defected microstructure, samples with a surfactant concentration of 1% v/v were selected for FTIR studies. All samples exhibit characteristic peaks of the pristine PCL spectra, including bands such as 2940 cm^{-1} and 2865 cm^{-1} (asymmetric and symmetric CH_2 stretching, respectively), 1722 cm^{-1} ($\text{C}=\text{O}$ stretching), 1294 cm^{-1} ($\text{C}-\text{C}$ and $\text{C}-\text{O}$ stretching), and 1240 cm^{-1} (asymmetric $\text{C}-\text{O}-\text{C}$ stretching) [11]. Moreover, the analysis of the chemical structure confirmed the presence of Triton X-100 in the material, as evidenced by the carbonyl band in the range of 1609 cm^{-1} , $\text{C}-\text{O}-\text{C}$ band at 1113 cm^{-1} , $\text{C}-\text{H}$ and $\text{C}-\text{C}$ stretching in an aromatic ring at 1510 cm^{-1} and band at 837 cm^{-1} typical for the structure of Triton X-100 [17]. On the other hand, a change in the ratio of the $1190\text{--}1160\text{ cm}^{-1}$ bands was observed in materials where Triton X-100/alanine emulsions were introduced into the fibers during the electrospinning process; however, none of these characteristic peaks were detected for Tween 80. This could be due to either overlapping characteristic bands of Tween 80 and PCL or too small amount of surfactant to be detected. Protein macromolecules encapsulated in micelles do not yield bands characteristic of the proteins used, and the fact that they cannot be detected on the surface indicates that they are trapped inside the fibers.

The outcomes are consistent with the results obtained by Jue Hu et al. where the core-shell fibers also showed the structure of a pristine PCL, without a trace of encapsulated biomolecules and surfactants [10]. The fact that in this study there are characteristic bands of Triton X-100 present in the FTIR spectra may result from the much higher concentration of the surfactant used in this experiment.

TABLE 1 presents the results of the contact angle measurements for the prepared membranes, which confirm that the addition of surfactants strongly affects the physicochemical properties of the fiber surface. The presence of surfactants, regardless of concentration, completely changed the wettability of PCL samples from hydrophobic ($\sim 130^\circ$) to highly hydrophilic ($\sim 20\text{--}35^\circ$). However, as the concentration of the surfactant increases, the contact angle decreases slightly. This could be attributed to the presence of a surfactant on the surface of the fibers. The effect was enhanced by the high humidity of the process ($\sim 50\%$) and a small amount of the water phase, which contributed to a more uniform distribution of the surfactant between oil-air and oil-water interfaces, since both were thermodynamically favourable for surfactant location. The same sharp decrease in the contact angle was also observed by Johnson et al. during their studies on emulsion electrospun PCL/Span 80/water fibrous mats [16].

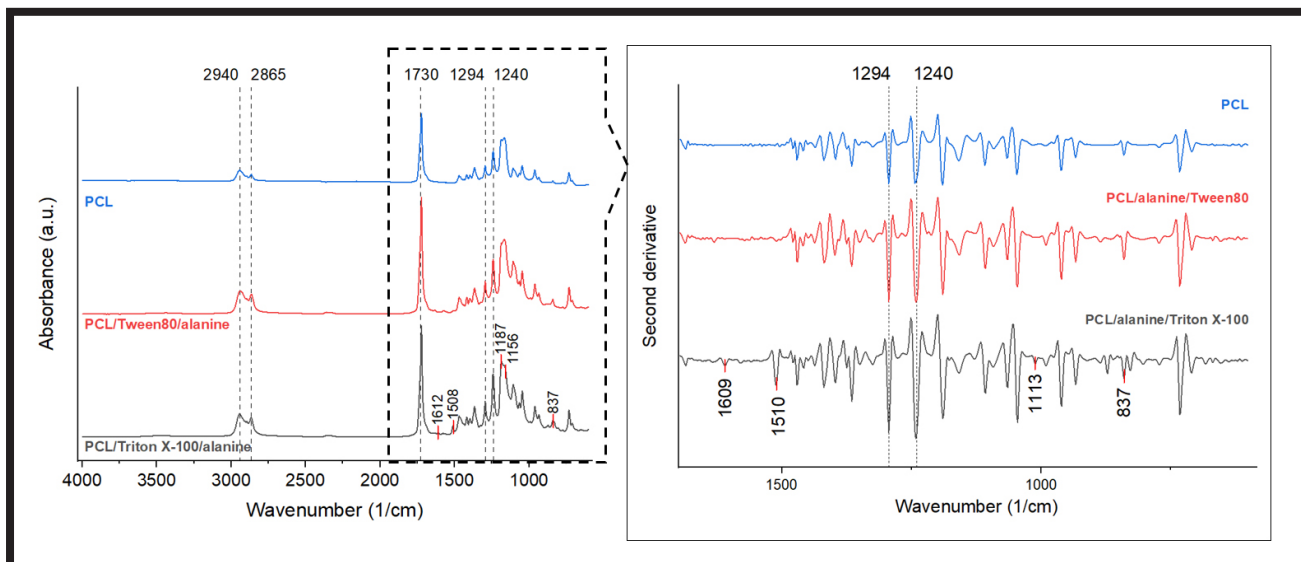


FIG. 3. FTIR spectra of the PCL, PCL/Tween80/alanine and PCL/Triton X-100/alanine using 1% Tween 80 and 1% Triton X-100.

TABLE 1. Contact angle of the electrospun fibers using emulsions with different content of the surfactants and loading efficiency of alanine.

Sample	Concentration of surfactant (%)	Loading efficiency of alanine (%)	Average contact angle (°)
PCL/Triton X-100/alanine	0.5	4.95	29.5 ± 3.7
	1	2.21	21.5 ± 2.7
	3	1.29	20.5 ± 4.8
PCL/Tween80/alanine	0.5	6.84	35.3 ± 5.2
	1	2.10	24.0 ± 3.9
	5	1.35	22.0 ± 2.5
PCL	-	-	128.8 ± 2.2

The analysis of spectrophotometric results (UV-Vis) confirms the continuous release of a small amount of alanine (up to ~0.7 mg) from the fibers over a period of 1 month (FIG. 4). Since the highest content of the surfactant resulted in a defected microstructure, the fibers obtained by emulsion electrospinning with the use of surfactants at a concentration of 1% were subjected to release studies. There were also no significant differences in the amount of alanine released or the release rate between PCL/Tween80/alanine and PCL/Triton X-100/alanine fibers, having similar fiber size. This means that the combination of core-shell morphology and uniform fiber size distribution influenced the release time of amino acid (alanine) and prevented the burst release phenomenon. Such a character of the curves indicates the mechanism of diffusion – erosion release of biomolecules. After the first day of incubation, an immediate increase in alanine concentration was observed due to the diffusion of water into the exposed pores containing the biomolecule. The subsequent constant increase in the concentration of alanine is associated with the slow erosion of the matrix, which led to the formation of small channels in the fibers leading to the migration of the active ingredient to the incubation solution [18].

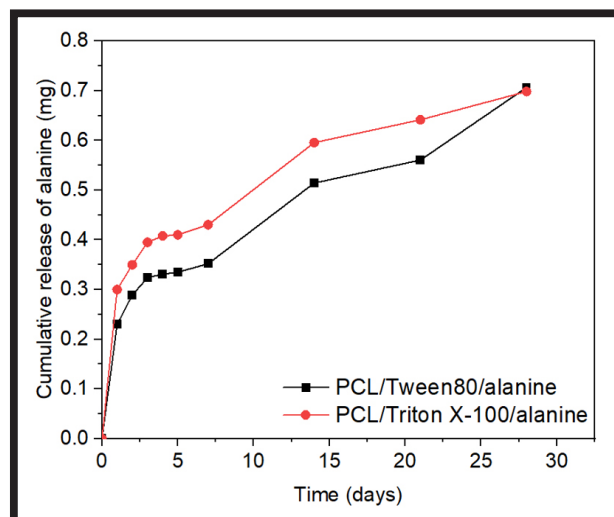


FIG. 4. Cumulative curve of alanine release from fibrous meshes prepared from emulsions PCL/Tween80/alanine and PCL/Triton X-100/alanine using 1% Tween 80 and 1% Triton X-100.

The observed release curves in FIG. 4 are difficult to clearly attribute to the mathematical models of Higuchi or Pappas-Kosmayer describing the kinetics of drug release (in DDS systems). In the case of fibers or microspheres, these limitations are mainly due to the form of the introduced drug (the need to use a drug in saturated form), which cannot always be used in this form due to the formulation process of the carrier [19]. Thus, in *in vitro* conditions, we have a combination of different mathematical models that allow us to describe the drug release profile. The most common drug release profile from polymeric drug delivery systems is the three-phase profile, which combines both effects related to drug diffusion and carrier erosion [20]. The work of Yin et al. showed that the diffusion-erosion mechanism is common to both fibers and microspheres [21]. Such a mechanism allows for the correlation of the drug release rate with degradation of the polymer matrix and to preserve the geometric shape of the fiber, and thus its role as a scaffold. However, due to the slow degradation rate of PCL, further studies of the release kinetics are required.





Conclusions

The emulsion electrospinning process allows to obtain fibers modified with micelles with biological compounds. By varying the concentration of surfactants, it was possible to obtain fibers with different morphology and diameter; however, excess amount of surfactant adversely affected both the microstructure and the surface of the fibers (increase in fiber diameter and surface roughness). In turn, the use of a lower concentration of surfactant resulted in obtaining more uniform and defect-free fibers. Furthermore, the addition of surfactants with encapsulated peptide increased the hydrophilicity of the fibers, which should be important for cell adhesion. The presence of the external polymer layer (shell part), as well as the differentiation of the internal porosity of the fibers, allowed for better control of the biomolecule release kinetics. The diffusion-erosion mechanism of release of biomolecules resulted in a prolonged release time and prevented burst release. The research results indicate that emulsion electrospinning is a promising method of encapsulating biological molecules, which can be used to stimulate tissue regeneration processes that require a specific approach, e.g. soft tissue. To confirm the potential of the obtained substrates as the vehicles for the biomolecule in further research, we will focus on optimizing the surfactant concentration, which will provide high cell viability.

Acknowledgement

This work was supported from the subsidy of the Ministry of Education and Science for the AGH University of Science and Technology in Kraków (Project No. 16.16.160.557).

ORCID iDs

R. Kurpanik:  <https://orcid.org/0000-0002-7943-7509>
 A. Rapacz-Kmita:  <https://orcid.org/0000-0001-8788-5144>
 A. Ścisłowska-Czarnecka:  <https://orcid.org/0000-0001-8398-8912>
 E. Stodolak-Zych:  <https://orcid.org/0000-0002-8935-4811>

References

- [1] M.P. Nikolova, M.S. Chavali: Recent advances in biomaterials for 3D scaffolds: A review. *Bioact. Mater.* 4 (2019) 271-292. <https://doi.org/10.1016/j.bioactmat.2019.10.005>.
- [2] K. Klimek, G. Ginalska: Proteins and peptides as important modifiers of the polymer scaffolds for tissue engineering. *Polymers (Basel)*. 12(844) (2020) 1-38. <https://doi.org/10.3390/polym12040844>
- [3] K. Hosoyama, C. Lazurko, M. Muñoz, C.D. McTiernan, E.I. Alarcon: Peptide-based functional biomaterials for soft-tissue repair. *Front. Bioeng. Biotechnol.* 7 (AUG) (2019) <https://doi.org/10.3389/fbioe.2019.00205>.
- [4] A.S. Walvekar, R. Srinivasan, R. Gupta, S. Laxman: Methionine coordinates a hierarchically organized anabolic program enabling proliferation. *Mol. Biol. Cell* 29 (2018) 3183-3200. <https://doi.org/10.1091/mbc.E18-08-0515>.
- [5] N. Ron-Harel, J.M. Ghergurovich, G. Notarangelo, M.W. LaFleur, Y. Tsubosaka, A.H. Sharpe, J.D. Rabinowitz, M.C. Haigis: T Cell activation depends on extracellular alanine. *Cell Rep.* 28(12) (2019) 3011-3021.e4. <https://doi.org/10.1016/j.celrep.2019.08.034>.
- [6] H. Frizzell, T. Ohlsen, K.A. Woodrow: Protein-loaded emulsion electrospun fibers optimized for bioactivity retention and pH-controlled release for peroral delivery of biologic therapeutics. *Int. J. Pharm.* 533(1) (2017) 99. <https://doi.org/10.1016/J.IJP-HARM.2017.09.043>.
- [7] A. Luraghi, F. Peri, L. Moroni: Electrospinning for drug delivery applications: A review. *J. Control. Release* 334 (2021) 463-484. <https://doi.org/10.1016/j.jconrel.2021.03.033>.
- [8] U. Angkawinitwong, S. Awwad, P.T. Khaw, S. Brocchini, G.R. Williams: Electrospun formulations of bevacizumab for sustained release in the eye. *Acta Biomater.* 64 (2017) 126-136. <https://doi.org/10.1016/j.actbio.2017.10.015>.
- [9] J. Wang, M. Windbergs: Controlled dual drug release by coaxial electrospun fibers – Impact of the core fluid on drug encapsulation and release. *Int. J. Pharm.* 556 (2019) 363-371. <https://doi.org/10.1016/J.IJP-HARM.2018.12.026>.
- [10] J. Hu, M.P. Prabhakaran, X. Ding, S. Ramakrishna: Emulsion electrospinning of polycaprolactone: Influence of surfactant type towards the scaffold properties. *J. Biomater. Sci. Polym. Ed.* 26 (1) (2015) 57-75. <https://doi.org/10.1080/09205063.2014.982241>.
- [11] C. Moura, M. Simões, I.C. Gouveia, B. Xu: Emulsion Electrospun Fiber Mats of PCL/PVA/Chitosan and Eugenol for Wound Dressing Applications. *Adv. Polym. Technol.* (2019) <https://doi.org/10.1155/2019/9859506>.
- [12] L. Ma, X. Shi, X. Zhang, L. Li: Electrospinning of polycaprolacton/chitosan core-shell nanofibers by a stable emulsion system. *Colloids Surfaces A Physicochem. Eng. Asp.* 583 (August) (2019) 123956. <https://doi.org/10.1016/j.colsurfa.2019.123956>.
- [13] A.O. Basar, S. Castro, S. Torres-Giner, J.M. Lagaron, H. Turkoğlu Sasmazel: Novel poly(ϵ -caprolactone)/gelatin wound dressings prepared by emulsion electrospinning with controlled release capacity of Ketoprofen anti-inflammatory drug. *Mater. Sci. Eng. C* 81 (2017) 459-468. <https://doi.org/10.1016/j.msec.2017.08.025>.
- [14] B. Baskapan, A. Callanan: Electrospinning fabrication methods to incorporate laminin in polycaprolactone for kidney tissue. *Tissue Eng. Regen. Med.* (2021) <https://doi.org/10.1007/s13770-021-00398-1>.
- [15] B. Arechabala, C. Coiffard, P. Rivalland, L.J.M. Coiffard, Y. De Roeck-Holtzauer: Comparison of cytotoxicity of various surfactants tested on normal human fibroblast cultures using the neutral red test, MTT assay and LDH release. *J. Appl. Toxicol.* 19 (3) (1999) 163-165. [https://doi.org/10.1002/\(SICI\)1099-1263\(199905/06\)19:3<163::AID-JAT561>3.0.CO;2-H](https://doi.org/10.1002/(SICI)1099-1263(199905/06)19:3<163::AID-JAT561>3.0.CO;2-H).
- [16] P.M. Johnson, K.E. Knewton, J.G. Hodge, J.M. Lehtinen, A.S. Trofimoff, D.J. Fritz, J.L. Robinson: Surfactant location and internal phase volume fraction dictate emulsion electrospun fiber morphology and modulate drug release and cell response. *Biomater. Sci.* 9 (4) (2021) 1397-1408. <https://doi.org/10.1039/d0bm01751e>.
- [17] V.R.N. Banu, V.R. Babu, S. Rajendran: Investigating the corrosion inhibition efficiency of surgical carbon steel instruments used in medical field. *Int. Res. J. Pharm.* 8 (12) (2018) 79-90. <https://doi.org/10.7897/2230-8407.0812254>.
- [18] U. Posadowska, M. Brzychczy-Włoch, E. Pamuła: Gentamicin loaded PLGA nanoparticles as local drug delivery system for the osteomyelitis treatment. *Acta Bioeng. Biomech.* 17 (3) (2015) 41-47. <https://doi.org/10.5277/ABB-00188-2014-02>.
- [19] J. Siepmann, N.A. Peppas: Higuchi equation: Derivation, applications, use and misuse. *Int. J. Pharm.* 418 (1) (2011) 6-12. <https://doi.org/10.1016/j.ijpharm.2011.03.051>.
- [20] N. Kamaly, B. Yameen, J. Wu, O.C. Farokhzad: Degradable controlled-release polymers and polymeric nanoparticles: Mechanisms of controlling drug release. *Chem. Rev.* 116 (4) (2016) 2602-2663. <https://doi.org/10.1021/acs.chemrev.5b00346>.
- [21] L. Yin, K. Wang, X. Lv, R. Sun, S. Yang, Y. Yang, Y. Liu, J. Liu, J. Zhou, Z. Yu: The fabrication of an ICA-SF/PLCL nanofibrous membrane by coaxial electrospinning and its effect on bone regeneration in vitro and in vivo. *Sci. Rep.* 7 (1) (2017) 1-12. <https://doi.org/10.1038/s41598-017-07759-8>.

NEW DESIGN OF PATIENT-SPECIFIC, ANTIMICROBIAL BIOACTIVE FINGER IMPLANTS FOR DURABLE FUNCTIONAL RECONSTRUCTION AFTER AMPUTATION

MARCIN DYNER, ADAM BYRSKI, ROMAN MAJOR,
MACIEJ GAWLIKOWSKI, KATARZYNA KASPERKIEWICZ,
JUERGEN M. LACKNER, ANETA DYNER,
BOGUSŁAW MAJOR

[*Engineering of Biomaterials* 161 (2021) 8-14]

doi:10.34821/eng.biomat.161.2021.8-14

In the originally published version of this manuscript, incorrect acknowledgements were provided.

Corrected as follows.

Acknowledgements

Parts of the reported results were derived from a cooperative M-ERA.NET project called "fingerIMPLANT", which is co-funded by the Polish National Centre of Research and Development, Grant no. fingerIMPLANT M-ERA.NET2/2019/7/2020, and the Austrian Research and Promotion Agency, Grant no. 878515. In the introduction, in Figure 1 on page 11 and in the article text partly project proposal text and results are presented, which were generated by the project partner Dr. David Lumenta and Dr. Andrzej Hecker, Medical University Graz, Dr. Martin Schwentenwein, Lithoz GmbH, Andreas Hinterer, MSc. and Sebastian Spalt, MSc., Inocon Technologie GmbH, and by the project coordinator JOANNEUM RESEARCH.

[*Engineering of Biomaterials* 162 (2021) 26]

doi:10.34821/eng.biomat.162.2021.26



Copyright © 2021 by the authors. Some rights reserved.
Except otherwise noted, this work is licensed under
<https://creativecommons.org/licenses/by/4.0>